

On the Habitability of Universes without Stable Deuterium

Fred C. Adams^{a,b}, and Evan Grohs^a

^a*Physics Department, University of Michigan, Ann Arbor, MI 48109*

^b*Astronomy Department, University of Michigan, Ann Arbor, MI 48109*

Abstract

In both stars and in the early universe, the production of deuterium is the first step on the way to producing heavier nuclei. If the strong force were slightly weaker, then deuterium would not be stable, and many authors have noted that nucleosynthesis would be compromised so that helium production could not proceed through standard reaction chains. Motivated by the possibility that other regions of space-time could have different values for the fundamental constants, this paper considers stellar evolution in universes without stable deuterium and argues that such universes can remain habitable. Even in universes with no stellar nucleosynthesis, stars can form and will generate energy through gravitational contraction. Using both analytic estimates and a state-of-the-art stellar evolution code, we show that such stars can be sufficiently luminous and long-lived to support life. Stars with initial masses that exceed the Chandrasekhar mass cannot be supported by degeneracy pressure and will explode at the end of their contraction phase. The resulting explosive nucleosynthesis can thus provide the universe with some heavy elements. We also explore the possibility that helium can be produced in stellar cores through a triple-nucleon reaction that is roughly analogous to the triple-alpha reaction that operates in our universe. Stars burning hydrogen through this process are somewhat hotter than those in our universe, but otherwise play the same role. Next we show that with even trace amounts (metallicity $Z \sim 10^{-10}$) of heavy elements — produced through the triple-nucleon process or by explosive nucleosynthesis — the CNO cycle can operate and allow stars to function. Finally, we consider Big Bang Nucleosynthesis without stable deuterium and find that only trace amounts of helium are produced, with even smaller abundances of other nuclei. With stars evolving through gravitational contraction, explosive nucleosynthesis,

the triple-nucleon reaction, and the CNO cycle, universes with no stable deuterium are thus potentially habitable, contrary to many previous claims.

Keywords: Fine-tuning; Multiverse; Stellar Nucleosynthesis

1. Introduction

The laws of physics allow for the development of life in our universe, but many authors have noted that sufficiently large variations could render the universe uninhabitable [1, 2, 3, 4, 5, 6, 7, 8]. One partial explanation for why the laws of physics have their observed form is that our universe is one out of many [9, 10]. This vast collection of universes — the multiverse — samples all of the possible versions of physical law. In this scenario, the strength of the strong force could be different in the various universes that make up the multiverse. If the strong force were stronger, however, then diprotons and dineutrons could be stable, and then nucleosynthesis would proceed in a different manner, although recent work shows that stars can still operate [11]. On the other hand, if the strong force were sufficiently weaker, then deuterium would not have a bound state. In a universe with no deuterium, the usual stepping stone on the pathway to heavy elements would not be available. Many authors have speculated that the absence of stable deuterium would lead to a universe with no heavy elements at all, and hence a lifeless universe [2, 3, 4, 12]. The goal of this paper is to explore the possibility that stars can provide both energy generation and nucleosynthesis, even in the absence of stable deuterium. Under the action of gravitational contraction alone, stars can generate enough energy, with sufficiently long lifetimes, for a universe to be habitable. For this scenario, massive stars will collapse at the end of their contraction phase and provide heavy elements through explosive nucleosynthesis. In addition, we explore the triple-nucleon reaction, which is analogous to the triple-alpha reaction that produces carbon in our universe. This type of reaction provides yet another pathway for the synthesis of heavy elements.

This type of alternate universe must still form stars in order to operate. In our universe, however, the star formation process is largely independent of nuclear considerations [13, 14], so that star formation could readily take place in the absence of stable deuterium. More specifically, the interstellar medium forms objects with a wide range of masses, and those entities have no way to tell in advance that their final masses should be capable of achieving

nuclear fusion. Moreover, the process of star formation often forms stellar-like bodies with masses that are too small to sustain nuclear reactions. These brown dwarfs are abundant in our universe, with about one such object for every 4 or 5 ordinary stars [15].

The vast majority of stars (those with masses less than about $7 M_{\odot}$ [16]) are born with stellar structure configurations that are too large in radius and too cool in central temperature to sustain nuclear reactions. After formation, these bodies slowly contract and are powered by the loss of gravitational potential energy. This contraction phase ends when the stellar core becomes sufficiently hot and dense for hydrogen fusion to take place. As a result, nuclear fusion occurs millions of years after the formation of most stars, defined here as hydrostatically supported objects that have been separated from the molecular clouds that produce them. High mass stars ($M_* > 7M_{\odot}$) follow a similar evolutionary path, but their contraction times are shorter than their formation times. These high mass objects are also powered by gravitational contraction in their earliest phases, but they transition into nuclear burning configurations before they attain their final masses.

In this paper, we assume that the star formation process proceeds as outlined above for our universe [13, 14], and consider the subsequent evolution of stars in the absence of stable deuterium. For this scenario, we explore four stellar processes that allow the universe to become potentially habitable: gravitational contraction, supernova-like explosions due to stellar collapse, the triple-nucleon reaction (analogous to the triple-alpha reaction that produces carbon in our universe), and finally hydrogen fusion through the CNO cycle. The following discussion outlines our treatment of each of these processes.

In the absence of nuclear reactions, the gravitational contraction phase described above for pre-main-sequence stars in our universe will continue over much longer spans of time. This paper shows that stars can generate enough energy, over sufficiently long timescales, to sustain life. In this scenario, small stars will contract until their central regions become degenerate, and their luminosities will slowly fade. For high mass stars, however, degeneracy pressure is not sufficient to support the mass of the star and it will experience catastrophic collapse. The subsequent implosion compresses the stellar core to enormous densities and temperatures so that explosive nucleosynthesis can take place, even in the absence of stable deuterium nuclei. The result is much like Type Ia supernovae in our universe, where these explosions are produced by the collapse of white dwarfs. As a result, low mass stars can

provide energy through gravitational contraction, whereas high mass stars can provide nucleosynthesis through collapse.

The mass scale that marks the boundary between high mass stars and low mass stars is the Chandrasekhar mass [17]. This scale represents the largest mass that can be supported by non-relativistic degeneracy pressure of electrons [18, 19, 20] and depends on the chemical composition of the object. For stellar evolution in our universe, the Chandrasekhar mass M_{Ch} is usually evaluated under the assumption that $A/Z = 2$, where Z is the atomic number and A is the atomic weight (because stars that become white dwarfs in our universe are mostly made of carbon and oxygen). For the first generation of stars in a universe without stable deuterium, the composition is expected to be pure hydrogen so that $A/Z = 1$. Since $M_{\text{Ch}} \propto (A/Z)^{-2}$ [17, 18, 19], the Chandrasekhar mass will be larger than in our universe, namely $M_{\text{Ch}} \approx 5.6M_{\odot}$.

Stars can also burn hydrogen through other reaction chains that do not rely on the existence of stable deuterium. We first consider the triple-nucleon reaction, which is analogous to the triple-alpha reaction that produces carbon in our universe. In this latter case, the ^8Be isotope is unstable, so the simplest reaction $^4\text{He} + ^8\text{Be} \rightarrow ^{12}\text{C}$ is suppressed. In spite of being unstable, ^8Be nuclei are produced in stellar cores due to nuclear statistical equilibrium (NSE). The production of ^8Be is not energetically favored because the isotope is unstable, so that the standing population is small. Nonetheless, enough ^8Be exists so that carbon can be produced. In a roughly similar scenario, deuterium nuclei will be produced in stellar cores, even though they are unstable and not energetically favored. Because of the inefficiency of the weak interaction, the stellar core will not generally reach NSE, so that the abundances of nuclear species must be calculated more explicitly. However, the resulting population of deuterium nuclei can interact with protons to form ^3He , which eventually fuses into ^4He . The abundance of deuterium is a steeply increasing function of temperature, so that this reaction requires stellar cores to be hotter and denser than their counterparts in hydrogen burning stars in our universe.

The final process that we consider is the Carbon-Nitrogen-Oxygen (CNO) cycle. In this chain of reactions, carbon is used as catalyst to fuse hydrogen into helium [18, 19]. Although no deuterium is required for this reaction chain, at least some carbon must be present. As a result, some previous epoch of nucleosynthesis, through collapse of high mass degenerate stars and/or through the triple nucleon reaction, must occur in order for this channel to be viable. This paper shows that the CNO cycle can operate —

and drive stellar evolution much like that in our universe — provided that the stellar metallicity $Z > 10^{-10}$. For comparison, the metallicity of the Sun $Z_{\odot} \approx 0.013$ [21] and the metallicity of the most metal-poor stars observed in the universe have at least $Z \sim 10^{-7}$ [22].

For the scenario considered here, with no stable deuterium, the universe is expected to emerge from its early epochs with essentially no elements heavier than hydrogen. During the first several minutes of cosmic time, during the epoch known as Big Bang Nucleosynthesis (BBN), our universe converts about one fourth of its mass into helium, with trace amounts of deuterium and lithium [23, 24]. Without stable deuterium as an intermediate state, this paper shows that BBN produces only traces amounts of helium, with mass fraction $X_4 \sim 10^{-14}$. We can thus assume that the first generation of stars have an almost pure hydrogen composition. Compared to the conditions realized during BBN, however, stellar cores can provide higher temperatures, higher densities, and longer time scales for confinement. These properties thus allow stars to achieve hydrogen fusion, even in the absence of stable deuterium.

This paper is organized as follows. Stellar evolution through gravitational contraction alone, with no nuclear burning, is considered in Section 2. The largest stars must collapse at the end of their contraction phase and can potentially produce heavier elements through explosive nucleosynthesis. The triple-nucleon process is considered in Section 3. After showing that stellar cores generally do not have time to reach NSE, we develop a generalized reaction network that keeps track of free neutrons. These reactions allow stars to generate energy and evolve much like stars in our universe, albeit with higher temperatures both in the core and on the surface. Next we show that stars with trace amounts of carbon can operate through the CNO cycle and this chain of nuclear reactions is explored in Section 4. For completeness, we revisit the epoch of Big Bang Nucleosynthesis in Section 5 and show that BBN produces essentially no heavy nuclei. The paper concludes, in Section 6, with a summary of our results and a discussion of their implications.

2. Stellar Evolution through Gravitational Contraction

In this section we consider the evolution of stars in the absence of any nuclear reactions. These stars will evolve through gravitational contraction (only) and can provide strategically situated planets with an ample supply of energy. In order to substantiate this claim, we use both analytic arguments

(Section 2.1) and numerical simulations from the *MESA* computational package (Section 2.2). In this scenario — with no sustained nuclear burning — the synthesis of heavy elements can take place during the collapse that marks the end of evolution for sufficiently massive stars (Section 2.3). Note that in this section we retain the constants (k, c, \hbar) , consistent with most literature on stellar structure. For the remainder of the paper, however, we set these constants to unity and work in natural units.

2.1. Gravitational Contraction of Non-burning Stars

Using the standard arguments with homology relations for the equations of stellar structure (see chapter 20 of [19]), we can find scaling relations for the luminosity as a function of stellar properties. For radiative stars using Kramer’s opacity law $\kappa \propto \rho T^{-7/2}$ [18, 19, 20], where ρ is density and T is temperature, one finds

$$L_* \sim L_0 \left(\frac{M_*}{M_0} \right)^{11/2} \left(\frac{R_*}{R_0} \right)^{-1/2} \left(\frac{\mu G}{\mu_0 G_0} \right)^{15/2}, \quad (1)$$

where L_* , M_* , R_* , and μ represent the stellar luminosity, mass, radius, and mean molecular weight. The subscript ‘0’ denotes reference values. For more massive stars that ionize their interiors, the stellar opacity is given by the Thompson cross section, and the scaling relation simplifies to the form

$$L_* \sim L_0 \left(\frac{M_*}{M_0} \right)^3. \quad (2)$$

Consider a newly formed star with no nuclear reactions and a relatively large mass $M_* > 1M_\odot$. At first, the star will be powered by gravitational contraction, just like pre-main-sequence stars operate in our universe. The gravitational energy is given by

$$U = -f_1 \frac{GM_*^2}{R_*}, \quad (3)$$

where f_1 is a dimensionless constant of order unity, so that the stellar luminosity is given by

$$L_* = \frac{dE}{dt} = -f_1 \frac{GM_*^2}{R_*^2} \frac{dR_*}{dt}. \quad (4)$$

As the star contracts, its central temperature and central density grow larger according to the scaling laws

$$T_C \propto \frac{1}{R_*} \quad \text{and} \quad \rho_C \propto \frac{1}{R_*^3}. \quad (5)$$

The central temperature is thus given by an expression of the form

$$kT_C = f_2 \frac{GM_* m_p}{R_*}, \quad (6)$$

where f_2 is another dimensionless constant of order unity, and m_p is the proton mass. The derivation of this relation assumes that the pressure is provided by the ideal gas law. This assumption breaks down under two conditions: [a] the star becomes too dense, so that degeneracy pressure dominates, and [b] the star is too massive, so that the pressure required to support the star leads to a temperature large enough that radiation pressure dominates.

For sufficiently massive stars, the central temperature thus has a maximum value given by the transition to an equation of state dominated by radiation pressure. This maximum value has been derived previously [25, 26] and has the form

$$kT_{\max} \approx 1.4 \left(\frac{m_{\text{ion}}}{\langle m \rangle} \right)^{8/3} m_e c^2 \approx 4.5 \text{ MeV}, \quad (7)$$

where m_{ion} is the mass of the nuclei and $\langle m \rangle$ is the mean mass per particle. Since we are considering massive stars with a pure hydrogen composition, $m_{\text{ion}} = m_p$ and $\langle m \rangle \approx m_p/2$ (assuming efficient ionization of the stellar interior). Note that electrons become relativistic at this energy scale. When electrons are relativistic, they produce less degeneracy pressure for a given density, and cannot support a star against catastrophic collapse. Stars with masses above the Chandrasekhar limit will eventually collapse and achieve this maximum temperature.

For stars with smaller masses ($M_* < M_{\text{Ch}}$), the onset of degeneracy enforces a maximum temperature in the stellar core. This maximum value has been derived previously [18, 20, 25] and can be written in the form

$$kT_{\max} = \frac{5}{36(4\pi)^{2/3}} \frac{G^2 M_*^{4/3} m_p^{8/3} m_e}{\hbar^2} \approx 5.8 \text{ keV} \left(\frac{M_*}{M_\odot} \right)^{4/3}. \quad (8)$$

The largest temperature that can be attained without the collapse of the stellar core is given by equation (8) for the Chandrasekhar mass. This temperature is ~ 60 keV or $\sim 7 \times 10^8$ K.

The contraction time is determined by the integration of equation (4). As shown above, the luminosity is nearly constant as the radius shrinks for sufficiently massive stars. The time required for the star to contract to a radius R_* is thus given by

$$\Delta t = f_3 \frac{GM_*^2}{L_* R_*}, \quad (9)$$

where f_3 is a dimensionless parameter of order unity. Since the star has a maximum temperature, it must have a minimum radius given by

$$R_{\min} = f_2 \frac{GM_* m_p}{kT_{\max}}. \quad (10)$$

Combining these equations we thus obtain

$$\Delta t = \frac{f_3}{f_2} \frac{M_*}{m_p} \frac{kT_{\max}}{L_*}. \quad (11)$$

For $M_* = 10M_\odot$, the luminosity $L_* \approx 10^4 L_\odot$, and the total evolution time becomes $\Delta t \approx 10^7$ yr. For stars with much larger masses, $M_* \gg 10M_\odot$, the luminosity scales as $L_* \sim M_*$, so that the time required to reach the maximum temperature is nearly the same for all massive stars. For stars in the mass range $M_{\text{Ch}} < M_* < 10M_\odot$, the stellar luminosity scales according to $L_* \sim M_*^3$, so that the total evolution time $\Delta t \sim M_*^{-2}$. Decreasing the stellar mass to M_{Ch} thus provides (only) a factor of three increase in Δt . As a result, all massive stars (with $M_* > M_{\text{Ch}}$) have evolution time scales of order 10 Myr.

For stars less massive than the Chandrasekhar mass ($\sim 5.6M_\odot$), the central regions never reach the point where electrons are relativistic. Instead they reach the maximum temperature given by equation (8). For stellar masses well below the Chandrasekhar mass, we can use this result to evaluate the time scale of equation (11), which leads to the result

$$\Delta t \approx 10^7 \text{ yr} \left(\frac{M_*}{M_\odot} \right)^{-2/3}, \quad (12)$$

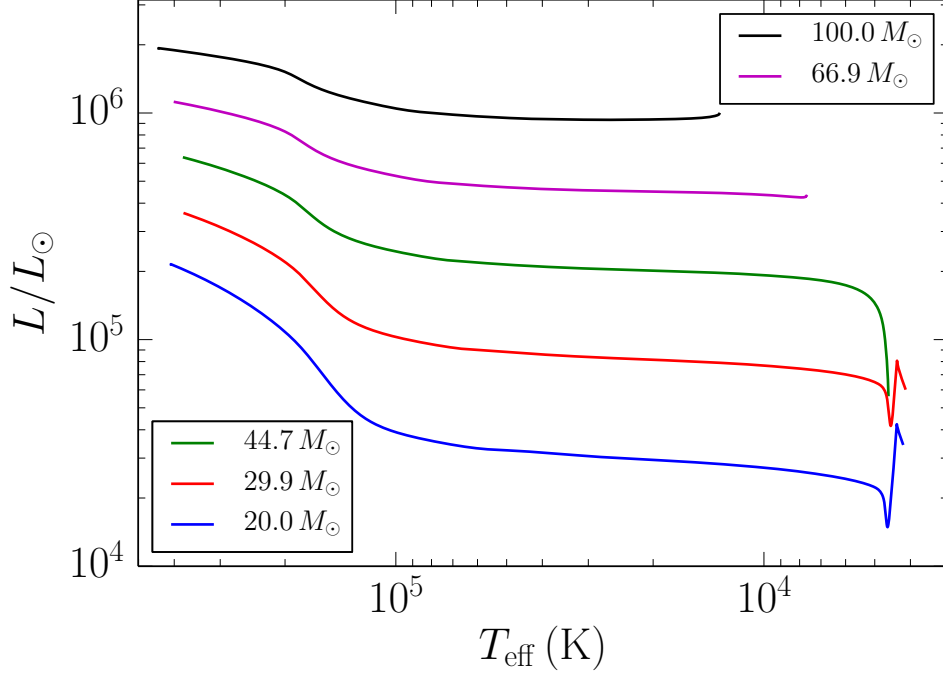


Figure 1: H-R diagram for stars in universes without stellar nucleosynthesis. The tracks illustrate the evolution of high mass stars with masses from $M_* = 20$ to $100 M_\odot$ (mass increases from bottom to top).

where we have used the luminosity scaling $L_* \sim M_*^3$. The evolution time is thus slowly varying. For sufficiently small stars, however, the interiors are not fully ionized, so that we must use the scaling relation of equation (1) instead of that of equation (2). With the steeper scaling relation $L_* \sim M_*^{11/2}$, the evolution time becomes longer.

2.2. Stellar Evolution Simulations without Nuclear Reactions

To illustrate the possible types of stellar evolution that can take place in universes with no deuterium, we first consider the case where no nucleosynthesis takes place in stars. Using the state-of-the-art computational package *MESA* [27, 28], we evolve a collection of stars under the action of gravitational contraction only. The stars are assumed to start in a configuration

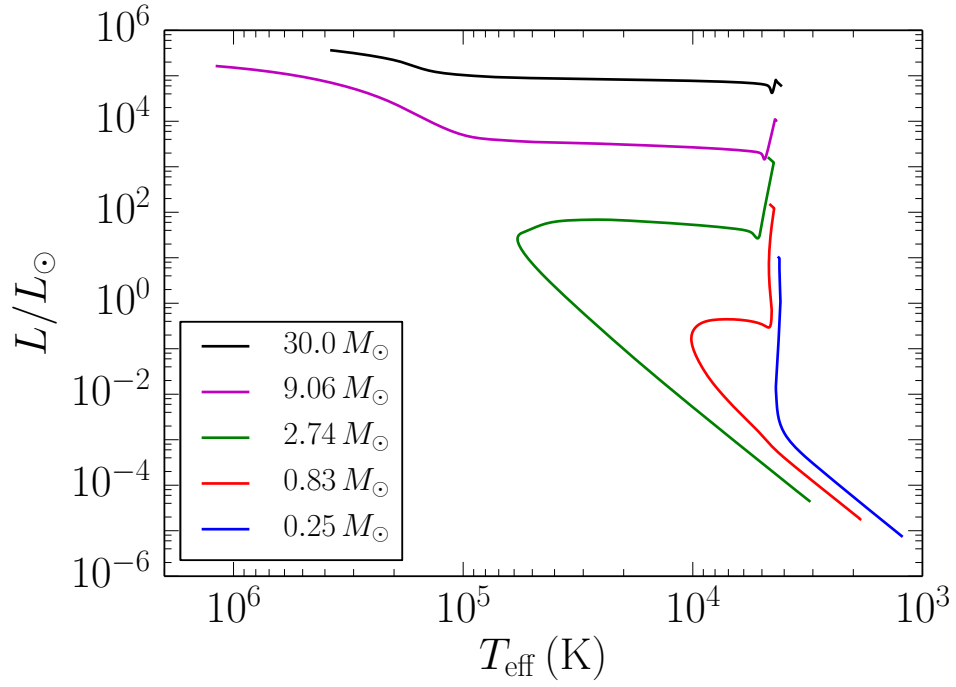


Figure 2: H-R diagram for stars in universes without stellar nucleosynthesis. The tracks illustrate the evolution of stars with varying masses from $M_* = 0.25 M_{\odot}$ (right-most blue track) to $30 M_{\odot}$ (upper-most black track).

comparable to the initial states for stars in our universe, i.e., with radii several times larger than their main-sequence sizes and correspondingly lower central temperatures [16]. The stars are also assumed to have zero metallicity with a pure hydrogen composition. The stars then evolve via gravitational contraction.

The evolution of these stars in the H-R diagram is illustrated in Figures 1 and 2. Evolutionary tracks are shown for a wide range of stellar masses, where $M_* = 0.25 - 100M_\odot$. Figure 1 shows the tracks for the upper end of the mass range (note that the luminosity scale is much smaller than that of Figure 2). In all cases, the stars begin with a nearly vertical track on the right side of the H-R diagram. During this early phase of evolution, the stellar interiors are convective, and gravitational contraction takes place at nearly constant effective temperature. For the high mass stars, this phase is short-lived ($\Delta t \sim 10^4$ yr), whereas low mass stars remain convective much longer ($\Delta t > 10^7$ yr). The process of star formation itself takes $\sim 10^5$ years, so that stars are not optically visible for the first part of the evolution shown here. Nonetheless, stars in our universe experience an analogous convective phase (except for massive stars with $M_* > 7M_\odot$, which evolve through their convective phase while they are still in the process of forming).

Following the convective phase, the stellar interiors become radiative and the tracks in the H-R diagram become nearly horizontal, corresponding to nearly constant luminosity (see equation [2]). In our universe, stars reach a central temperature where hydrogen fusion takes place and gravitational contraction halts. In the case considered here, with no nuclear reactions, the contraction continues. This relatively long-lived phase of constant luminosity is conducive to supporting habitable planets. The lifetime of this phase is given approximately by equation (11) for stars that are massive enough to remain radiative and have hot enough interiors so that the stellar opacity is given by the Thompson cross section. These conditions require the stars to be at least as massive as the Sun. For smaller stars, the interior is not fully ionized, and the opacity is given by Kramer's law. Under these conditions, where the luminosity is given by equation (1), the time spent on the horizontal evolutionary track becomes shorter. For stars less massive than $\sim 0.5M_\odot$, the stellar interior tends to stay convective for most of the stellar lifetime. These smaller stars tend to evolve directly from their convective tracks to their degenerate tracks. As a result, although small stars have long total lifetimes, the time spent in the radiative phase, with relatively constant luminosity, is shorter.

To illustrate the trends described above, Figure 3 plots the effective habitability time for stars as a function of their stellar mass. This habitability time is defined differently for high mass and low mass stars. For low mass stars, the stellar core reaches a maximum temperature when the star becomes dense enough to become dominated by degeneracy pressure. At this point in its evolution, the stellar luminosity decreases and the track in the H-R diagram follows the trend appropriate for white dwarfs in our universe. This turning point thus marks the end of the phase with nearly constant luminosity. We also note that the time spent in the early convective phase (depicted by the nearly vertical tracks in the H-R diagram) is short compared to the total. Larger stars have too much mass to be supported by degeneracy pressure. These stars also reach central temperatures and densities where electrons are degenerate. In these stars, however, the electrons are relativistic and cannot provide enough pressure to hold up the star. At this point in evolution, the high mass stars transition from gradual gravitational contraction to rapid gravitational collapse. These latter stages of collapse are short, so that the lifetime shown in Figure 3 represents the total evolutionary time of the star. The boundary between the two types of behavior described here occurs at the Chandrasekhar mass, where $M_{\text{Ch}} \approx 5.6M_{\odot}$ for stars composed of pure hydrogen. Notice, however, that the habitability time, as plotted in Figure 3, does not show a sharp boundary at the Chandrasekhar mass. Stars with masses somewhat less than M_{Ch} display the scaling law $\Delta t \propto M_*^{-2}$ expected for stars with $M_* > M_{\text{Ch}}$.

Figures 2 and 3 show that stars can provide substantial luminosity, at a relatively constant value, over time scales longer than 1 Gyr. For a star with mass $M_* = 0.8 M_{\odot}$, for example, the luminosity due to gravitational contraction is just under $1 L_{\odot}$ over a time of just under 1 Gyr. The total evolutionary times are even longer, although the luminosities fall with time. These considerations suggest that stars powered by gravitational contraction are sufficient as the required energy sources for habitability. In order for life to develop, however, some process must also drive nucleosynthesis. We also note that the luminosities of these stars are not as constant as those for hydrogen-burning stars in our universe. It would be useful to know how much variability can be tolerated and still allow for habitability.

Figure 4 shows the central temperature and density for a collection of stars with a range of masses. We note that the evolution is significantly different for stars above and below the Chandrasekhar mass, where $M_{\text{Ch}} \approx 5.6M_{\odot}$ for pure hydrogen. For stars with masses $M_* < M_{\text{Ch}}$, the central

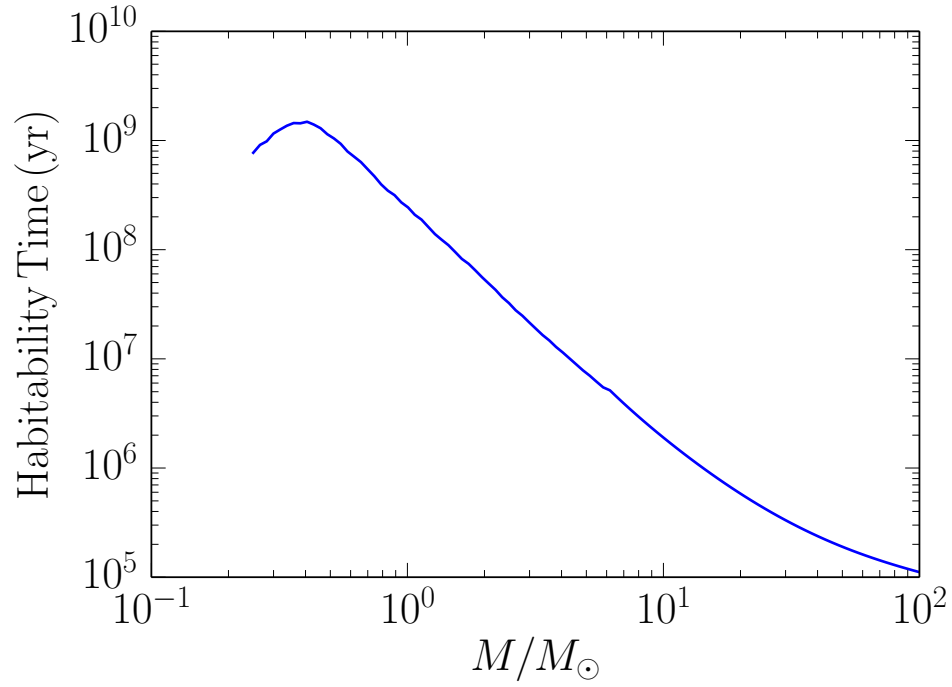


Figure 3: Effective time for habitability for stars powered by gravitational contraction only. The lifetime shown here corresponds to the time before the stars become degenerate. High mass stars quickly collapse after this point in evolution, whereas low mass stars slowly fade and follow white-dwarf-like tracks in the H-R diagram (see Figure 2).

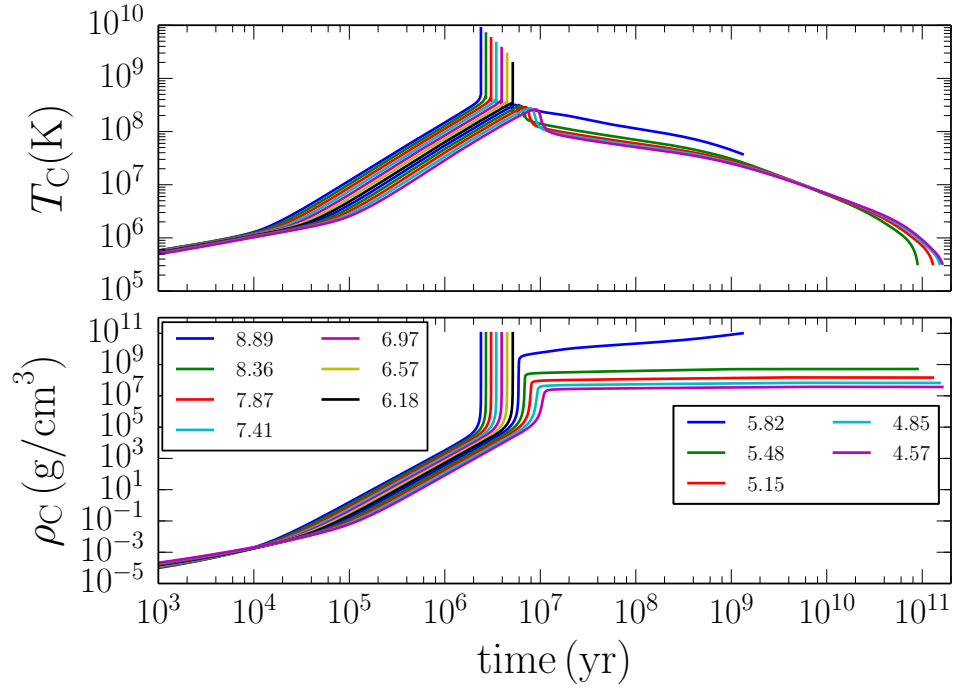


Figure 4: Central temperature and central density as a function of time for stars powered by gravitational contraction only. The various curves correspond to a range of masses, as labeled (in units of solar masses), both above and below the Chandrasekhar mass (where $M_{\text{Ch}} = 5.6M_{\odot}$ for stars with a pure hydrogen composition).

temperature rises steadily for ~ 10 Myr and then reaches a maximum value of order $T_{\text{max}} \sim 10^8$ K. This maximum temperature varies with stellar mass and is given by equation (8) to good approximation. For the largest mass, $M_* = M_{\text{Ch}}$, the maximum temperature $T_{\text{max}} \approx 7 \times 10^8$ K. At this time, the central density reaches a corresponding maximum value of order $\rho_{\text{C}} \sim 10^9$ g cm $^{-3}$. At this evolutionary stage, the star is supported by the non-relativistic degeneracy pressure of its electrons. At later times, the central temperature falls as the stellar core cools, whereas the central density remains nearly constant. The cooling time for the degenerate objects is relatively long (up to a *several* Gyr [29]), which allows the stars to remain relatively luminous and leads to the lifetimes shown in Figure 3.

For more massive stars, $M_* > M_{\text{Ch}}$, the time development of the central temperatures and densities follow trajectories similar to those of low mass stars up to times $t \sim \text{few}$ Myr. Instead of being supported by degeneracy pressure at this stage, however, these heavier stars transition from a state of relatively slow contraction to more rapid collapse. Both the central temperature and density increase sharply. The curves in Figure 4 become nearly vertical, indicating that collapse takes place quickly, with extremely little additional time elapsed. These stars are expected to collapse until they reach extreme densities so that they either become black holes and/or experience explosive nucleosynthesis, analogous to collapsing degenerate objects in our universe. For the evolutionary tracks presented here, however, the *MESA* code is unable to follow stars after the densities exceed $\rho_{\text{C}} \sim 10^{11}$ g cm $^{-3}$. At this stage, the central temperatures are of order $T_{\text{C}} \sim 10^{10}$ K ≈ 0.86 MeV, comparable to the mass difference between the proton and neutron (1.29 MeV). At these enormous temperatures, weak interactions (e.g., $e^- + p \rightarrow n + \nu_e$) are no longer suppressed and nuclear reactions take place readily. We thus expect nucleosynthesis to occur efficiently during the collapse of these stars, even in the absence of stable deuterium.

Figure 4 shows that the time evolution of central temperature and density proceeds differently for high mass stars and low mass stars. However, the boundary between stars that collapse and those that are supported by degeneracy pressure does not seem to occur at the quoted value of the Chandrasekhar mass $M_{\text{Ch}} = 5.6M_{\odot}$. Instead, stars of slightly larger mass (e.g., $M_* = 5.82M_{\odot}$ in the Figure) do not collapse in the simulations. The Chandrasekhar mass is derived assuming that the stellar structure is given exactly by an $n = 3/2$ polytrope [17], which applies in the limit where the stellar material is completely degenerate and has zero temperature. In contrast, the

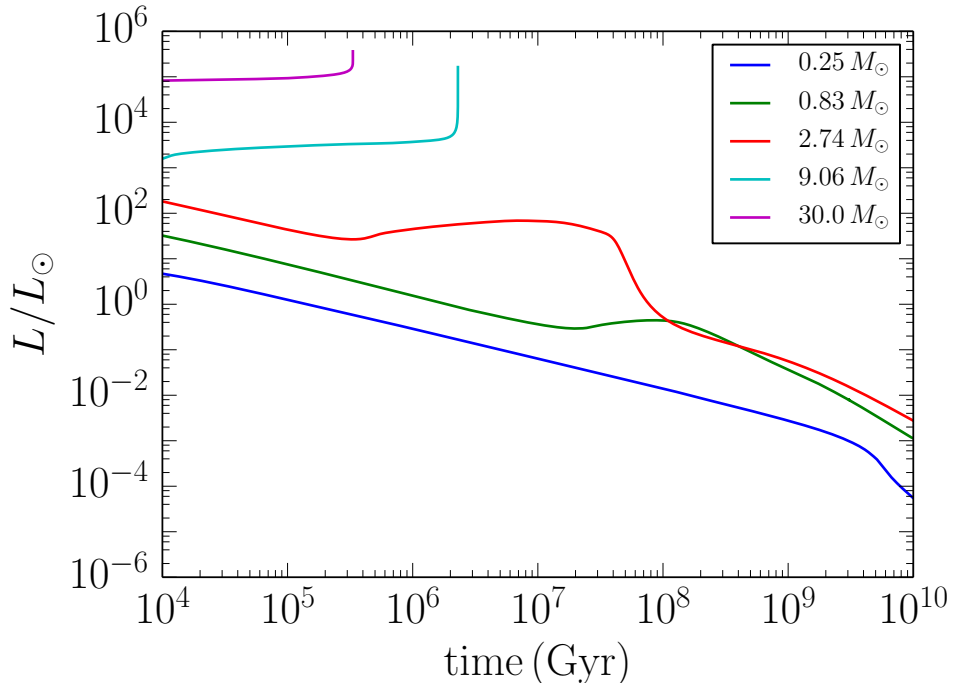


Figure 5: Luminosity as a function of time for stars powered by gravitational contraction only. The various curves correspond to a range of masses, as labeled, both above and below the Chandrasekhar mass.

stars in the simulations depicted in Figure 4 are not pure polytropes. This departure delays their collapse. If the simulations were continued to much longer times, the stellar material would eventually cool enough to become fully degenerate. In that limit, all stars with masses $M_* > M_{\text{Ch}}$ are expected to collapse.

The stellar luminosity is plotted as a function of time in Figure 5. The stars show three different types of behavior. For high mass stars, above the Chandrasekhar limit, the luminosity is roughly constant with time until the central regions become both relativistic and degenerate. At this point, the stars experience core collapse and the luminosity spikes upward. The total evolutionary time for these massive stars is short, $\Delta t < 10^7$ yr. For the smallest stars, roughly those with mass $M_* < 0.5 M_\odot$, the luminosity slowly

decreases over the entire stellar lifetime. These small stars are convective over their entire lifespan, until they become degenerate, and have no radiative phase. For stars with intermediate masses, roughly in the range $0.5M_{\odot} < M_* < M_{\text{Ch}}$, the luminosity decreases during an early convective phase, but then goes through a radiative phase with slowly varying luminosity. After the stars become degenerate, their luminosity decreases again.

The corresponding tracks in the H-R diagram for these stars are shown in Figure 2, which provides the surface temperatures of the stars in addition to their luminosity. Over the phases of nearly constant luminosity for stars with intermediate masses, the surface temperature steadily increases (see the nearly horizontal tracks in Figure 2). For a given stellar luminosity L_* and surface temperature T_* , the stellar radius R_* can be determined through the usual photospheric outer boundary condition $L_* = 4\pi R_*^2 \sigma T_*^4$. The stellar radius thus decreases while the surface temperature increases, such that the luminosity remains nearly constant. The tracks in the H-R diagram show that the surface temperature reaches a maximum value and then decreases. After this point, the stellar luminosity, temperature, and radius all decrease with time.

Figure 5 indicates that the largest stars with $M_* > M_{\text{Ch}}$ have short lifetimes (< 10 Myr) and are not good candidates to host potentially habitable planets. The smallest stars with $M_* < 0.5M_{\odot}$ have sufficiently long lifetimes, but exhibit steadily decreasing luminosity. As a result, the most promising stars for hosting planets are those with intermediate masses. These stars have substantial luminosity over relatively long spans of time. For example, stars with mass $M_* = 1 - 3M_{\odot}$ have luminosity $L_* > 0.07L_{\odot}$ over time scales longer than ~ 1 Gyr. The luminosity subsequently decreases steadily after this epoch. The onset of steadily declining power can thus be used to mark the end of the habitable phase, although this boundary is not sharp. Even these latter stars are not ideal — although the lifetimes are long and the luminosities are large, the luminosities are not as steady as those in our universe. As a point of comparison, the faint early Sun had a luminosity that was only smaller by $\sim 25\%$, but that change might have led to Earth freezing over. The variations in luminosity for the stars considered in this section vary to a greater degree and thus make habitability more difficult.

2.3. Explosive Nucleosynthesis

The previous section shows that stars with masses greater than the Chandrasekhar mass continue to contract under the action of gravity until their

cores reach enormous temperatures and densities (Figure 4). The properties of these stellar cores ($T > 10^{10}$ K and $\rho > 10^{11}$ g cm $^{-3}$) are similar to the conditions reached during Type Ia supernovae in our universe (e.g., see Figure 1 of Ref. [30]) so that explosive nucleosynthesis is expected to occur [31, 32]. However, the production of any complex nuclei must proceed by first producing deuterium (or another two-particle state) and then adding additional nucleons.

In our universe, the temperatures reached in the stellar cores are high enough that nuclear statistical equilibrium (NSE) can be realized [33, 34]. In NSE, nuclear reactions are in detailed balance, and the high densities help enforce this condition. The mass fractions of the various nuclear species are determined by minimizing the Helmholtz free energy. As a result, high entropy environments favor populations of lighter particles such as protons, neutrons, and helium. Low entropy environments favor the production of larger nuclei, those with the highest binding energy.

Although NSE provides a useful framework to estimate nuclear abundances, nuclear reactions can take place out of equilibrium. Moreover, NSE can only be reached if all of the relevant reactions proceed fast enough. As shown in the following section, however, the reaction rates for deuterium production are generally not fast enough for the stellar core to reach NSE conditions (see Section 3.1). In this case, deuterium can still be produced, and large nuclei are synthesized, but the abundances must be determined by more detailed calculations (see Section 3.2), rather than the standard statistical argument. In any case, the stellar core will support a (small) standing population of deuterium, even though the nuclei are unstable. These deuterium nuclei can interact further to produce larger nuclei, which are stable, and thereby jump-start the process of nucleosynthesis.

Although a detailed calculation of the nuclear yields for this scenario is beyond the scope of this present paper, we can provide a basic plausibility argument. The maximum temperature reached during the collapse phase of massive stars is given by equation (7). Significantly, this benchmark temperature ($T_{\text{max}} \approx 4.5$ MeV) is larger than three important energy scales: [1] twice the electron rest mass (1.02 MeV), [2] the mass difference between the proton and the neutron (1.29 MeV), and [3] the mass difference between (unstable) deuterium nuclei and the corresponding constituent particles (expected to be of $\sim 1-2$ MeV). As the temperature in the stellar core increases, pair production becomes efficient, and the population of both neutrons and deuterons will become significant due to considerations of nuclear statistical

equilibrium. As a result, nuclear reactions will not necessarily be suppressed due to the lack of a stable state for deuterium. The subsequent nucleosynthesis will then take place explosively as the star continues to contract. In the end, heavy elements will be produced and released into the background galaxy by the explosion.

For this scenario, it is important to note that explosive nucleosynthesis can only operate over a limited range of parameter space, where the masses and binding energies fall within a small neighborhood of those in our universe. The ordering of energy scales outlined above requires that the mass difference between the proton and neutron, and the nuclear binding energies, are of order 1 MeV. In general, nuclear physics does not require that the binding energies of nuclei (both positive and negative) must be comparable to the electron mass or to the temperatures reached during stellar implosions. As a result, universes with nuclear binding energies sufficiently different from ours will not achieve explosive nucleosynthesis as outlined here. In addition, although we consider unstable deuterium, we are also assuming that nuclei with three nucleons ($A = 3$), as well as ${}^4\text{He}$, are bound.

When explosive nucleosynthesis is operative, the resulting nuclei can be incorporated into subsequent generations of stars.¹ If these nuclei are primarily helium, then later stellar generations can process them into carbon, which is useful both for biology and for running the CNO cycle in those stars (see Section 4). If the explosion directly produces carbon and heavier elements, then the metallicity of the galaxy will steadily increase, and later generations of stars will also be able to operate via the CNO cycle.

For completeness, we note that the temperature does not have to reach the maximum value T_{max} in order for some nuclear processing to take place. In general, the abundance of deuterium is expected to be suppressed by the multiplicative factor $\exp[-\Delta_d/T]$, where Δ_d is a measure of the degree to which deuterium fails to be bound (see Section 3.1). Since we are considering scenarios where $\Delta_d \sim 1$ MeV, as long as the temperature is not too far below this value, some deuterium will be present and some nuclear reactions will occur. However, once the density reaches the extremely large values depicted in Figure 4, the time scale for further collapse becomes short. In order to produce a standing population of deuterium, weak interactions must

¹We are implicitly assuming that stars are forming and evolving inside a galaxy, and that the explosion is contained within its gravitational potential well.

be operative. As a result, the production of deuterium can be suppressed due to the slow rate of weak interactions.

3. Stellar Evolution through Triple-Nucleon Reactions

In the absence of stable deuterium, the synthesis of protons into helium can take place through triple-nucleon reactions that are roughly analogous to the triple-alpha process that produces carbon in our universe [18, 19]. For the triple-alpha process, the transient population of unstable beryllium is determined by Nuclear Statistical Equilibrium (NSE), so that we first consider the limiting case where unstable deuterium arises in NSE (Section 3.1). Because of the slow reaction rates and rapid decay of deuterium, however, we find that NSE is generally not reached. As a result, a more general treatment is developed by keeping track of the population of free neutrons (Section 3.2). The resulting reactions produce a transient population of deuterium that can interact to produce ^3He and eventually ^4He . The evolution of stars under the action of triple-nucleon processes is presented in Section (3.3).

3.1. Nuclear Statistical Equilibrium

In this section, we consider the simplest case where a standing population of deuterium is produced in NSE, and estimate the properties required for the system of reactions to reach equilibrium. At sufficiently high temperatures, the following reactions take place:

$$p + p \rightarrow {}^2\text{He} + \gamma \quad (13)$$

and

$${}^2\text{He} \rightarrow d + e^+ + \nu_e, \quad (14)$$

where ${}^2\text{He}$ is the diproton and d is the deuterium nucleus. Since the positron in this reaction will quickly find an electron and be annihilated, we are left with a net reaction of the form

$$e^- + p + p \rightarrow d + \gamma + \gamma + \nu_e. \quad (15)$$

Both the intermediate diproton nucleus (${}^2\text{He}$) and deuterium (${}^2\text{H}$) are unstable under the assumptions considered in this paper. However, these species will be present with some abundance due to nuclear statistical equilibrium (NSE). We note that for analogous reasons, evolved stars in our universe have

a standing population of ${}^8\text{Be}$, even though that nucleus is unstable. Most of the time, the diproton and the deuteron will decay back to their constituent particles. Nonetheless, some deuterium will interact before decaying via the reaction

$$p + d \rightarrow {}^3\text{He} + \gamma. \quad (16)$$

In our universe, this latter reaction produces an energy of 5.5 MeV: the binding energy of helium-3 is ~ 7.7 MeV, whereas the binding energy of deuterium is ~ 2.2 MeV. Here we assume that ${}^3\text{He}$ is stable with a comparable binding energy, and that deuterium is unstable.

In order to estimate the reaction rate for triple-nucleon processes, we must first find the expected abundance of unstable deuterium. In equilibrium, the chemical potentials must be equal on both sides of this equation so that

$$\mu_e + 2\mu_p = \mu_d. \quad (17)$$

Note that the chemical potential is zero for the photon and is assumed here to be zero for the neutrino. We also use the usual condition for kinetic equilibrium, which expresses the number density n_X of species X in the form

$$n_X = g_X \left(\frac{m_X T}{2\pi} \right)^{3/2} \exp \left[\frac{\mu_X - m_X}{T} \right], \quad (18)$$

where g_X is the number of internal degrees of freedom. If we use equation (18) to determine the chemical potentials of the protons and deuterium in reaction (15), the condition of chemical equilibrium from equation (17) takes the form

$$n_d = n_p^2 \left(\frac{g_d}{g_p^2} \right) 2^{3/2} \left(\frac{2\pi}{m_p T} \right)^{3/2} \exp \left[\frac{2m_p - m_d + \mu_e}{T} \right]. \quad (19)$$

To evaluate the chemical potential of the electron, we again invoke the condition of kinetic equilibrium (18) and the condition of charge neutrality, which implies that $n_e = n_p$. We obtain

$$\exp[\mu_e/T] = \exp[m_e/T] n_p g_e^{-1} \left(\frac{2\pi}{m_e T} \right)^{3/2}. \quad (20)$$

Using this result in equation (19), we find the following expression for the abundance of deuterium

$$n_d = n_p^3 \left(\frac{g_d}{g_e g_p^2} \right) 2^{3/2} \frac{(2\pi)^3}{(m_p m_e)^{3/2} T^3} \exp \left[\frac{2m_p + m_e - m_d}{T} \right]. \quad (21)$$

Here we define

$$\Delta_d \equiv m_d - (2m_p + m_e). \quad (22)$$

Since deuterium is unbound, $m_d > m_p + m_n > 2m_p + m_e$, so that Δ_d is a positive quantity. Although the quantity Δ_d could take a wide range of values, we are interested in the case where $\Delta_d = \mathcal{O}(1 \text{ MeV})$. In this regime, deuterium fails to be bound by an energy increment that is comparable to its actual binding energy in our universe. For much larger values of Δ_d , we expect the binding energies of other relevant nuclei (e.g., helium-4) to change significantly.

For convenience we define the scaled quantities

$$T_9 = \frac{T}{10^9 \text{ K}} \quad \text{and} \quad n_{30} = \frac{n_p}{10^{30} \text{ cm}^{-3}}, \quad (23)$$

where the benchmark values are chosen to be comparable to the central temperatures and densities realized by stars undergoing gravitational contraction (see Figure 4). We also assume that the stars are pure hydrogen so that $n_p = n$. The abundance of deuterium in NSE is thus given by

$$\chi_d = \frac{n_d}{n_p} = 2.3 \times 10^{-3} n_{30}^2 T_9^{-3} \exp \left[-11.63 \frac{\Delta_{\text{mev}}}{T_9} \right], \quad (24)$$

where we have also defined $\Delta_{\text{mev}} = \Delta_d / (1 \text{ MeV})$. For example, if we fix $\Delta_{\text{mev}} = 1$ and $n_{30} = 1$, then at high temperatures $T_9 = 1$, we find a deuterium abundance of $\chi_d \approx 2 \times 10^{-8}$. In spite of the seemingly small value, this deuterium abundance would lead to robust nuclear reactions. In our universe, the reaction rate for $p + d \rightarrow {}^3\text{He}$ is larger than that of $p + p \rightarrow d$ by a factor of $\sim 10^{18}$. As long as the deuterium abundance is larger than about 10^{-18} , nuclear reactions can proceed fast enough to support the star.

The time required for the central core of a star to reach NSE is determined by the slowest reaction rate. For the abundance of deuterium, the forward reaction is much slower than the decay of (unstable) deuterium back into its constituent parts. For the reaction of interest $pp \rightarrow d$, the cross section can be written in the form

$$\langle \sigma v \rangle_{pp} = 6.34 \times 10^{-39} \text{ cm}^3 \text{ sec}^{-1} T_9^{-2/3} f(T_9) \exp \left[-3.380 T_9^{-1/3} \right], \quad (25)$$

where T_9 is defined by equation (23) and where we have defined a function

$$f(T_9) = 1 + 0.123 T_9^{1/3} + 1.09 T_9^{2/3} + 0.938 T_9. \quad (26)$$

The reaction rate $\Gamma = n_p \langle \sigma v \rangle_{pp}$ and the corresponding time scale $\tau_{pp} = 1/\Gamma$ can be written in the form

$$\tau_{pp} \approx 1.6 \text{ yr } n_{30}^{-1} \exp \left[3.380 T_9^{-1/3} \right], \quad (27)$$

where we have used the benchmark value $T_9 \approx 1$ to evaluate the polynomial part of the expression. Using this same value in the exponential, we find a time scale $\tau_{pp} \approx 47 \text{ yr}$ (for $n_{30} = 1$). This time scale is shorter than the time scales for gravitational contraction ($\tau = 1 - 10 \text{ Myr}$), but much longer than the decay time for deuterium and the half-life of the neutron. As a result, NSE will not be maintained under most circumstances.

We can also illustrate the difficulty in reaching NSE by considering the equilibrium abundance of deuterium and comparing it to the NSE value given by equation (24). The net production rate for deuterium is given by

$$\frac{dn_d}{dt} = \frac{1}{2} n_p^2 \langle \sigma v \rangle_{pp} - \lambda_d n_d + \dots, \quad (28)$$

where λ_d is the decay rate for deuterium. Here we assume that the lifetime is comparable to that for ^8Be in our universe, so that $\lambda_d^{-1} \sim 10^{-16} \text{ s}$. Equation (28) neglects additional terms corresponding to the burning of deuterium into other nuclei. These reactions take place on astrophysical time scales and can be neglected for purposes of estimating equilibrium abundances. In steady state, the time derivative $dn_d/dt = 0$, so that the equilibrium abundance of deuterium is given by

$$n_d = \frac{1}{2} n_p^2 \langle \sigma v \rangle_{pp} \lambda_d^{-1}. \quad (29)$$

Using the values $T_9 = 1$ and $n_{30} = 1$, the density of deuterium becomes $n_d \approx 3 \times 10^4$, with a corresponding abundance $\chi_d = n_d/n_p \approx 3 \times 10^{-26}$. Since this value is much smaller than the NSE value found in equation (24), the system cannot maintain equilibrium. As a result, the abundance of deuterium must be determined out of equilibrium. This issue is addressed in the following section.

3.2. Triple-Nucleon Process including Free Neutrons

In the previous section, we considered the abundance of unstable deuterium in NSE and found that the required reaction rates are generally too slow to reach equilibrium. This section considers an alternate mechanism to bridge the $A = 2$ mass gap in a universe without stable deuterium. As

outlined above, unstable deuterium will be produced, even if the decay rate is too rapid for the system to reach NSE. These decays of deuterium follow the chain of reactions

$$d \rightarrow p + n \rightarrow p + p + e^- + \bar{\nu}_e, \quad (30)$$

which occur quickly compared to evolutionary time scales of stars. The second step in the path (30) is free-neutron decay, which has a mean lifetime $\tau_n = 885.1\text{s}$ in our universe [35, 36]. The neutron lifetime τ_n is indeed short compared to the lifetime of typical stars, but is long compared to nuclear reaction time scales, implying that the free neutrons from equation (30) could participate in nuclear reactions. In this section, we move beyond the assumption of NSE and determine how stellar interiors evolve with a reservoir of free neutrons.

In the presence of free neutrons, ${}^3\text{He}$ can be synthesized from three free nucleons through a reaction of the form

$$n + p + p \rightarrow {}^3\text{He} + \gamma. \quad (31)$$

We call this process the triple-nucleon reaction. In analogy with the triple-alpha reaction [37], we write the rate of production of ${}^3\text{He}$, $dY_3/dt|_+$, from reaction (31) as

$$\left. \frac{dY_3}{dt} \right|_+ = Y_n Y_p^2 \frac{\rho_b^2 N_A^2}{2\Gamma(d)} \langle np \rangle \langle dp \rangle, \quad (32)$$

where Y_i is the abundance of species i , ρ_b is the baryon mass density, $\Gamma(d)$ is the radiative decay width of unstable deuterium, and $\langle np \rangle$ and $\langle dp \rangle$ are the integrated products of cross section multiplied by speed ($\langle \sigma v \rangle$) for the reactions $n(p, \gamma)d$ and $d(p, \gamma){}^3\text{He}$, respectively. Note that equation (32) is written in natural units. We will take the radiative decay width $\Gamma(d)$ to be a parameter in our model. In our universe, ${}^8\text{Be}$ has a width $\Gamma({}^8\text{Be}) = 6.8\text{eV}$, and so we will consider decay widths for deuterium with comparable values. For the two $\langle \sigma v \rangle$ quantities, we will take the known cross section of $n(p, \gamma)d$ from Ref. [24], and that of $d(p, \gamma){}^3\text{He}$ from the *MESA* library.² Unlike the triple-

²For completeness, we note that there exists a reaction similar to that of equation (32) in our universe, namely $d(p, n)2p$, which has a known cross section $\langle \sigma v \rangle$ [38]. The reverse channel of this reaction thus corresponds to the synthesis of three individual nucleons into heavier bound states. However, this work does not use the corresponding value of $\langle \sigma v \rangle$ for $2p(n, p)d$ from Ref. [38] because the final state does not contain ${}^3\text{He}$ and because deuterium is unstable in this current scenario.

alpha reaction, we will assume only thermal non-resonant production of ${}^3\text{He}$ through reaction (31). With the absence of a resonance in the triple-nucleon reaction, the ‘binding energy’ of deuterium (denoted $B_d = m_d - m_p - m_n$) does not enter into the expressions for $\langle np \rangle$ and $\langle dp \rangle$. Furthermore, the expression for the production rate in equation (32) does not contain an explicit dependence on B_d . There may exist an implicit dependence of the radiative decay width on B_d , but we do not consider such models here. Therefore, our expression in equation (32) is independent of B_d . In addition, the reverse photo-dissociation reaction, $\gamma + {}^3\text{He} \rightarrow p + p + n$, contains dependence on binding energies. However, as the sum of the three individual nucleons is less massive than a deuteron and a proton, there is no intermediate state with deuterium. As a result, only the binding energy of ${}^3\text{He}$ ($B_3 \simeq 7.7\text{ MeV}$) is relevant in the reverse rate.

In order for the triple-nucleon reaction to operate in stars, some pathway must be able to convert free protons into free neutrons. The weak interaction offers a pathway through a modified form of the p - p reaction

$$p + p \rightarrow d + e^+ + \bar{\nu}_e, \quad (33)$$

$$d \rightarrow p + n. \quad (34)$$

The above endothermic reaction chain converts two protons into one proton and a neutron. With the available neutron, the triple-nucleon reaction from equation (31) can take place in stars. Given the stellar time scales and the languidness of the triple-nucleon reaction, we also must allow for the neutron to decay into a proton. We modify the nuclear network of the stellar code *MESA* in regard to the following reactions

$$p + p \rightarrow p + n + e^+ + \nu_e, \quad (35)$$

$$n \rightarrow p + e^- + \bar{\nu}_e, \quad (36)$$

$$n + p + p \leftrightarrow {}^3\text{He} + \gamma. \quad (37)$$

For reaction (35), we use the identical $\langle \sigma v \rangle$ in our universe for the reaction $p(p, e^+ \nu_e)d$, and demand that the final state is a neutron and proton instead of a deuteron. For neutron decay, we simply set the rate equal to $1/\tau_n$. The triple-nucleon reaction uses the expression in equation (32) for $\langle \sigma v \rangle$.

3.3. Stars Powered by the Triple-Nucleon Process

To illustrate the evolution of stars operating via the triple-nucleon reaction, we first present the results from the simulation of a $M_* = 15 M_\odot$ star with zero initial metallicity. The radiative decay width of deuterium is set to $\Gamma(d) = 10.0$ eV. All of these results were obtained using modified versions of the *MESA* computational package [27, 28]. For these simulations, the p - p chain is replaced by the reactions described in the previous section and the CNO cycle is inoperative, but the higher order (e.g., helium burning) reactions are the same as those in our universe. Figure 6 shows the evolution of the mass fractions for a variety of nuclei as a function of time, where the values are averaged over the total volume of the star. Similar to stars in our universe, the abundances of ^4He , ^{12}C , and ^{16}O rise and fall with increasing time, as different nuclear reactions become important. In addition, there is a standing population of ^3He which is continuously incorporated into ^4He , and replenished by the triple-nucleon reaction.

One interesting feature of the evolution shown in Figure 6 is the presence of a sea of neutrons, which have an mass fraction of order $X_n \sim 10^{-11}$, averaged over the total volume of the star. In this model, the transmutation of a free neutron only has two pathways: incorporation into a ^3He nucleus via the triple-nucleon reaction or beta-decay into a free proton. Once heavier elements are present (e.g., ^{12}C or ^{16}O), free neutrons could capture on the larger Z nuclei. The result of this process would be to slow the synthesis of ^3He . However, we did not include any neutron capture reactions in the model used in Figure 6. In addition, we did not include a two-neutron variant of the triple-nucleon reaction within *MESA*. The neutron abundance is so small that the contribution of $2n(p, \gamma)^3\text{H}$ is insignificant. Similarly, we did not include a three-proton variant of the triple-nucleon reaction. That reaction would require the weak interaction and would be slower than the npp reaction once the free neutrons have a standing population.

Next we consider the evolution of stars in the H-R diagram operating through the triple-nucleon reactions from Section 3.2. Figure 7 shows a comparison of the tracks in the H-R diagram for stellar models with mass $M_* = 15M_\odot$. The solid blue, dashed red, dash-dot green, and dotted black curves depict the evolution of stellar models using the triple-nucleon reaction with varying values of the decay width $\Gamma(d) = 1 - 10^3$ eV. We terminate the evolutionary tracks after the mass fraction of metals in the stellar core reaches 50% (where metals are defined to be all nuclei with $A > 5$).

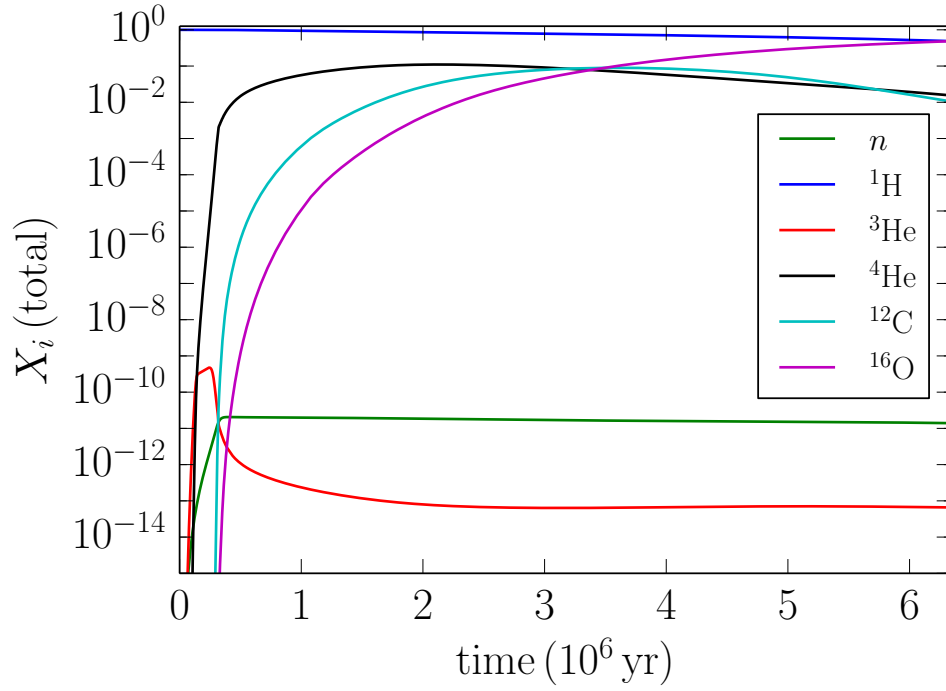


Figure 6: Mass fractions versus time for a $15 M_{\odot}$ star in a universe without stable deuterium. The initial metallicity of the star is zero. The model employed here uses the set of reactions (35) – (37) with $\Gamma(d) = 10.0 \text{ eV}$ to synthesize ^3He .

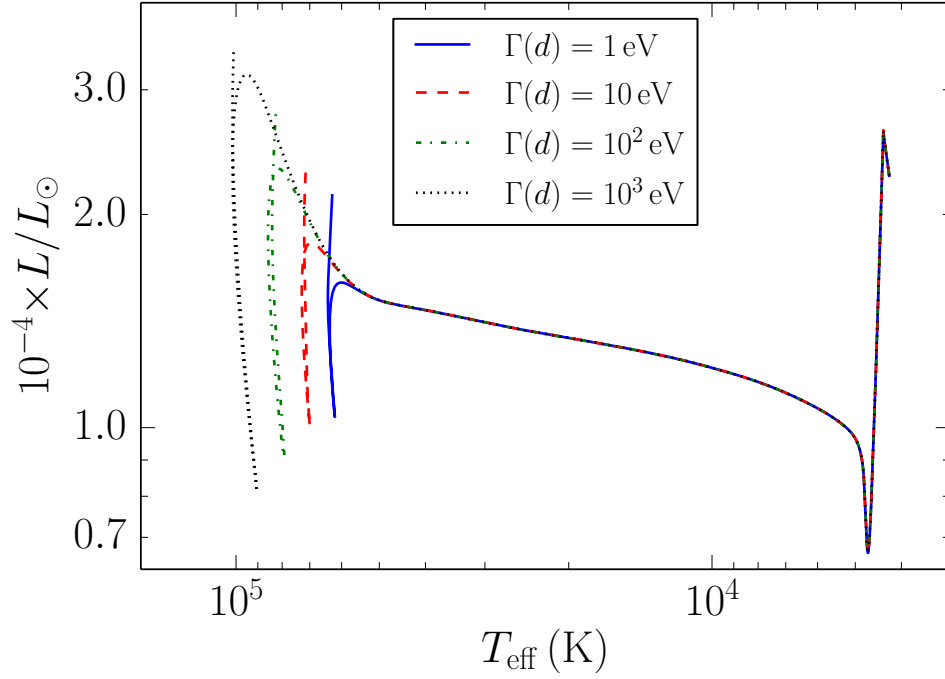


Figure 7: Evolutionary tracks in the H-R diagram for a $15 M_{\odot}$ star in a universe without stable deuterium. The tracks show the results for different values of the parameters that specify the triple-nucleon reactions. The four curves follow the evolution in the diagram for the triple-nucleon model of Section 3.2 for various values of the width $\Gamma(d)$.

The stellar models illustrated in Figure 7 show broadly similar evolution with some interesting differences. All of the models follow essentially the same tracks in the H-R diagram for the beginning phases of evolution. The tracks continue until the central core of the star is hot enough for enough hydrogen fusion to occur rapidly enough — through the triple-nucleon process — to support the star against further contraction. The surface temperature at the onset of nuclear burning depends on the decay width $\Gamma(d)$. Larger values of the width $\Gamma(d)$ correspond to faster decay of deuterium, which in turn require higher central temperatures for sustained nuclear reactions and produce correspondingly higher surface temperatures. The luminosity of the star also tends to increase with increasing values of the decay width $\Gamma(d)$, although the variation is relatively small (a factor of ~ 2) and the tracks move up and down in luminosity with time. Notice also that a $15 M_{\odot}$ star in our universe has luminosity $L_* \sim 10^4 L_{\odot}$, roughly comparable to the luminosities displayed in Figure 7.

4. Stellar Evolution including the CNO Cycle

Another way for stars to generate energy in the absence of stable deuterium is through the CNO cycle. This chain of reactions requires somewhat higher temperature and density than the p - p reaction chain, but it does not require a stable deuterium nucleus as an intermediate state. On the other hand, the cycle only operates with a minimum abundance of the element carbon, where the requisite values are determined below. As a result, some carbon nuclei must be produced by alternative means, either through explosive nucleosynthesis during the collapse of stellar cores or through the triple-nucleon process (and subsequent triple-alpha process). As we show here, however, the required carbon abundance can be much smaller than the typical values in our universe.

In this section, we first present our treatment of the CNO cycle (Section 4.1) and then show how stars can evolve with no deuterium and trace amounts of carbon via the CNO cycle (Section 4.2). We then consider how stars evolve during the action of both the triple-nucleon process and the CNO cycle (Section 4.3) and finally present a comparison of the different scenarios for hydrogen burning considered in this paper (Section 4.4).

4.1. The CNO Reaction Chain

With non-zero abundances of carbon, the CNO cycle proceeds through the following set of nuclear reactions:



Note that the reactions (39) and (42) represent beta decay. Use of this particular set of reactions implicitly assumes that the beta decays have time to occur before the parent nuclei interact further. This approximation is valid for stellar nucleosynthesis in the solar core. In the present context, the reaction rates are likely to be smaller (than in our universe) due to the reduced abundances of the CNO nuclei. In the event that the star in question has enough of these elements, and high enough temperature and density, so that the CNO reactions proceed rapidly, the star can generate energy through additional sets of nuclear reactions. For this present treatment, we focus on the simpler case corresponding (only) to reactions (38) to (43).

The slowest reaction in the CNO cycle is given by equation (41) for $^{14}\text{N} + p \rightarrow ^{15}\text{O}$. This reaction thus determines the overall rate at which energy is generated. The net energy generation rate for the entire cycle can then be written in the form

$$\epsilon_{\text{CNO}} \approx 10^{26} \text{ erg g}^{-1} \text{ sec}^{-1} \rho X_H X_C T_9^{-2/3} \exp \left[-\frac{15.23}{T_9^{1/3}} \right], \quad (44)$$

where X_C is the mass fraction of carbon. For comparison, the energy generation rate for the p - p chain can be written in the form

$$\epsilon_{pp} \approx 10^4 \text{ erg g}^{-1} \text{ sec}^{-1} \rho X_H^2 T_9^{-2/3} \exp \left[-\frac{3.381}{T_9^{1/3}} \right]. \quad (45)$$

As a point of comparison, we can equate these two expressions and find the conditions required for the CNO cycle to provide as much energy the p - p chain does for stars in our universe. We thus find

$$10^{22} X_C = X_H \exp \left[\frac{11.85}{T_9^{1/3}} \right]. \quad (46)$$

The largest temperature that can be achieved in a star — in the absence of collapse — is given by equation (8) for a given stellar mass. This equation assumes that the stars are below the Chandrasekhar mass limit ($M_*/M_\odot < 5.6$), but it provides a good benchmark for all stellar masses. Using this result, and taking $X_H = 1$, the required carbon mass fraction can be written in the form

$$\log_{10} X_C \approx -22 + 12.7(M_*/M_\odot)^{-4/9}. \quad (47)$$

For the largest star that can be supported by degeneracy pressure, and hence does not collapse, the mass $M_*/M_\odot \approx 5.6$ and the minimum required carbon abundance $X_C \approx 10^{-16}$. For a solar mass star, the minimum carbon abundance is larger, $X_C \approx 5 \times 10^{-10}$. Note that these abundances are much smaller than those corresponding to Solar metallicity. This difference arises because the stars in question can achieve maximum temperatures $T \sim 7 \times 10^8$ K, which are much larger than the operating temperature of solar-type stars.

4.2. Stars Powered by the CNO Cycle

To illustrate the effectiveness of the CNO cycle, we have run the *MESA* stellar evolution code for the following scenario. Deuterium is assumed to be unstable. As a result, the standard p - p chain of reactions (which powers low-mass stars in our universe) is assumed to be inoperative. In order to isolate the viability of the CNO cycle, we also assume that the triple-nucleon reaction (see Section 3) is not working. The metallicity of the star is taken to be small, $Z = 10^{-8}$. By definition, the value of Z determines the mass fraction of all elements heavier than helium. For the sake of definiteness, we assume that the relative abundances of these elements are the same as the cosmic abundances in our universe, although the mass fraction of carbon is the crucial quantity. In addition, we set the initial mass fraction Y of helium to be zero, so that we are implicitly assuming that Big Bang Nucleosynthesis is also ineffective. This low but nonzero value of Z could be produced, for example, by an early generation of massive stars that evolve through gravitational contraction (Section 2) and then explode as supernovae when

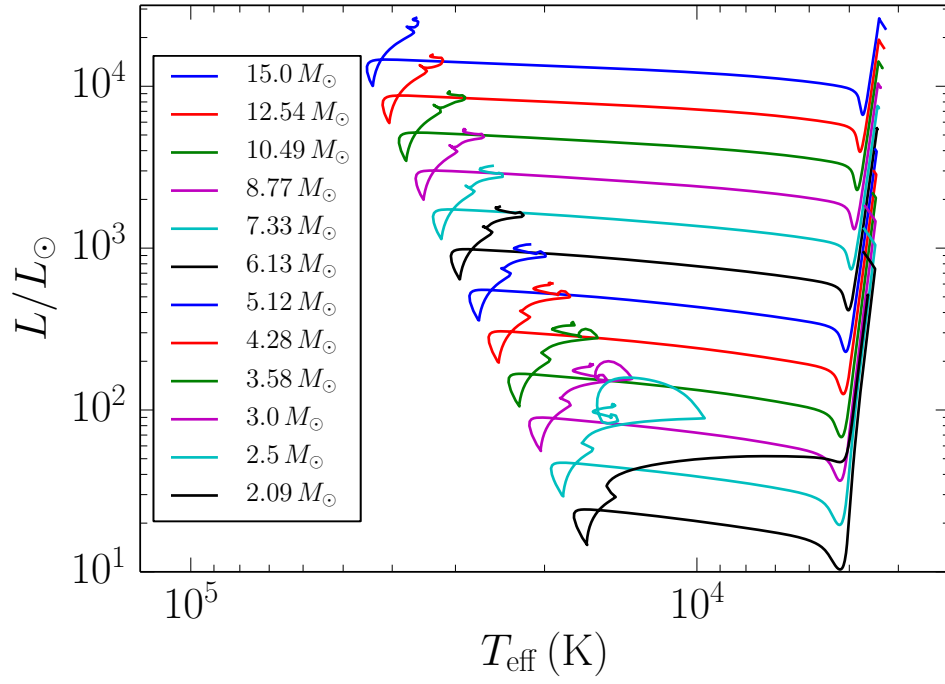


Figure 8: H-R diagram for stars evolving under the action of the CNO cycle with metallicity $Z = 10^{-8}$. In this scenario, both the p - p chain and the triple-nucleon process are assumed to be inoperative. The ends of the evolutionary tracks correspond to configurations where the mass fraction of elements with $A > 5$ exceeds 50% in the stellar core.

they enter into their collapse phase after a few Myr (Figure 4). A metallicity $Z = 10^{-8}$ requires about 100 solar masses of carbon for a galaxy with mass comparable to the Milky Way.

Under the conditions outlined above, the evolution of the stars in the H-R diagram is shown in Figure 8. The evolution is much like those of stars in our universe. The stars begin with fully convective interiors, so that they first contract on nearly vertical tracks in the H-R diagram. After becoming radiative, the stars then evolve on nearly horizontal tracks; they move to the left in the H-R diagram, with increasing surface temperatures, until hydrogen burning commences through the CNO cycle. The onset of nucleosynthesis produces a well-defined main sequence over the range of stellar masses, as delineated by the left boundary of the envelope of tracks shown in Figure 8. Note that the formation timescale for stars is of order 0.1 Myr. For high mass stars, with $M_* > 7M_\odot$, the time required for the stars to evolve to a hydrogen burning configuration is shorter than the formation time, so that these stars will first become optically visible with their main-sequence properties.

The resulting main-sequence for these CNO stars is characterized by somewhat higher luminosity and significantly higher surface temperatures compared to stars in our universe. The low metallicity requires the stars to contract to higher central temperatures for the CNO cycle to operate (see equation [46]) and also leads to lower overall opacity. This latter property allows radiation to escape from the star more readily and requires the stars to be hotter and brighter, for a given stellar mass, than stars with ordinary metallicity (e.g., $Z \sim Z_\odot \sim 0.02$). To explore this issue further Figure 9 shows the zero-age main-sequence for stars with varying metallicity in the range $Z = 10^{-6} - 10^{-10}$. As the value of Z decreases, the main-sequence falls farther to the left in the H-R diagram. This trend reflects the higher surface temperatures for stars with little metals, as indicated by equation (47).

These CNO-only stars burn hotter than those in our universe and thus have a correspondingly shorter main-sequence lifetime (although the lifetime is still longer than that for stars with no nuclear reactions, as shown in Figure 3). The low values of metallicity considered here apply only to the first generation of stars. After finishing their hydrogen burning phase (via the CNO cycle), sufficiently massive stars will continue to evolve and produce ever-heavier elements, analogous to how stellar evolution takes place in our universe. Subsequent generations of stars will thus have higher metallicity and will appear quite similar to those in our universe. The key issue is not the stability of deuterium, but rather the existence of bound states for a

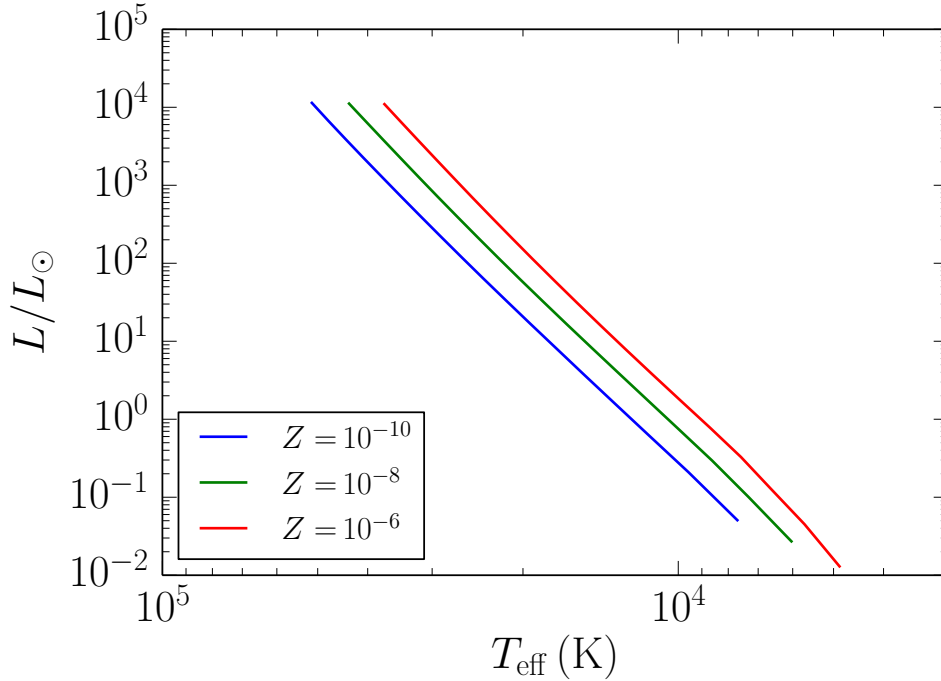


Figure 9: H-R diagram for stars of varying metallicity evolving under the action of the CNO cycle only. The curves show the Zero-Age Main-Sequence (ZAMS) for stars with metallicity $Z = 10^{-6}$ (red), 10^{-8} (green), and 10^{-10} (blue). For this scenario, both the p - p chain and the triple-nucleon process are assumed to be inoperative.

suite of heavier elements. The element carbon is especially important, as it is usually considered as the basis for life and, in this context, plays a vital role in catalyzing nuclear reactions in stars.

4.3. Combined Triple-Nucleon Process and CNO Cycle

We now consider the evolution of stars where both the triple-nucleon process and the CNO cycle are operational. Figure 10 shows the resulting tracks in the H-R diagram for three stars of different masses, each starting at zero metallicity. We employ the set of reactions (35) – (37) with $\Gamma(d) = 10.0$ eV to initially synthesize ${}^3\text{He}$ (and subsequently ${}^4\text{He}$) from free protons. We also include the reactions from the CNO cycle (see Section 4.1) in this

model. The labels on the H-R track for the $15 M_{\odot}$ star correspond to various burning regimes. First, the triple-nucleon reaction burns single nucleons into ${}^3\text{He}$. At the point labeled *npp*, the star has burned 1% of the ${}^1\text{H}$ in its core into ${}^3\text{He}$. The ${}^3\text{He}$ is incorporated into ${}^4\text{He}$, which is burned into ${}^{12}\text{C}$. Once there is a substantial population of ${}^{12}\text{C}$ available, the CNO cycle more efficiently burns ${}^1\text{H}$ into ${}^4\text{He}$. At the point labeled CNO, the reaction luminosity (power output for a given set of reactions integrated over the total volume of the star) for CNO surpasses that of the triple-nucleon reaction. Towards the end of the track, we label the point 3α when the mass fraction of ${}^{12}\text{C}$ accounts for more than 1% of the core. ${}^{12}\text{C}$ is required for the CNO cycle to operate. As we started with zero metallicity, the triple-alpha reaction must produce ${}^{12}\text{C}$ before the CNO cycle commences. We labeled 3α after CNO to show the regimes where each reaction or set of reactions dominates, but the 3α reaction is actually in operation before the labeled point in the HR track. The CNO cycle requires very little ${}^{12}\text{C}$ to operate. Indeed, at the point labeled CNO, the mass fraction of ${}^{12}\text{C}$ in the core is $X_{12} \simeq 3 \times 10^{-14}$.

4.4. Comparison of the Nuclear Models

Figure 11 shows the Zero-Age Main-Sequences (ZAMS) for the different nuclear models considered in this work. For the sake of definiteness, we define the ZAMS to be when 5% of the initial ${}^1\text{H}$ has been synthesized into heavier elements. The mass range depends on the specific model and parameter value. CNO models only employ the CNO cycle to synthesize ${}^4\text{He}$ from free protons. Those models depend on the initial metallicity parameter, Z , and are shown in Figure 11 as solid lines. Decreasing the metallicity slows the CNO reactions and pushes the ZAMS to higher effective temperatures. In addition, the stellar mass required for CNO burning increases with decreasing Z . For $Z = 10^{-6}$, $0.5 M_{\odot}$ stars are able to burn ${}^1\text{H}$. For $Z = 10^{-10}$, stars must have larger masses, upwards of $0.72 M_{\odot}$. As a result, the curve marking the ZAMS for low metallicity Z is not as long as that for higher Z in Figure 11. The CNO models do not require as high of temperatures as the triple-nucleon models, at least for large masses. Those models show that increasing the radiative decay width, $\Gamma(d)$, raises the temperatures needed for ${}^1\text{H}$ burning. Similar to the trends for the CNO models, increasing $\Gamma(d)$ raises the minimum stellar mass required for ${}^1\text{H}$ burning. The lowest mass plotted for the $\Gamma(d) = 1.0 \text{ eV}$ model is $M_* = 0.72 M_{\odot}$, as opposed to $1.0 M_{\odot}$ for $\Gamma(d) = 10^3 \text{ eV}$. Notice that for small masses, the triple-nucleon reaction with $\Gamma(d) = 1.0 \text{ eV}$ is competitive with the CNO cycle.

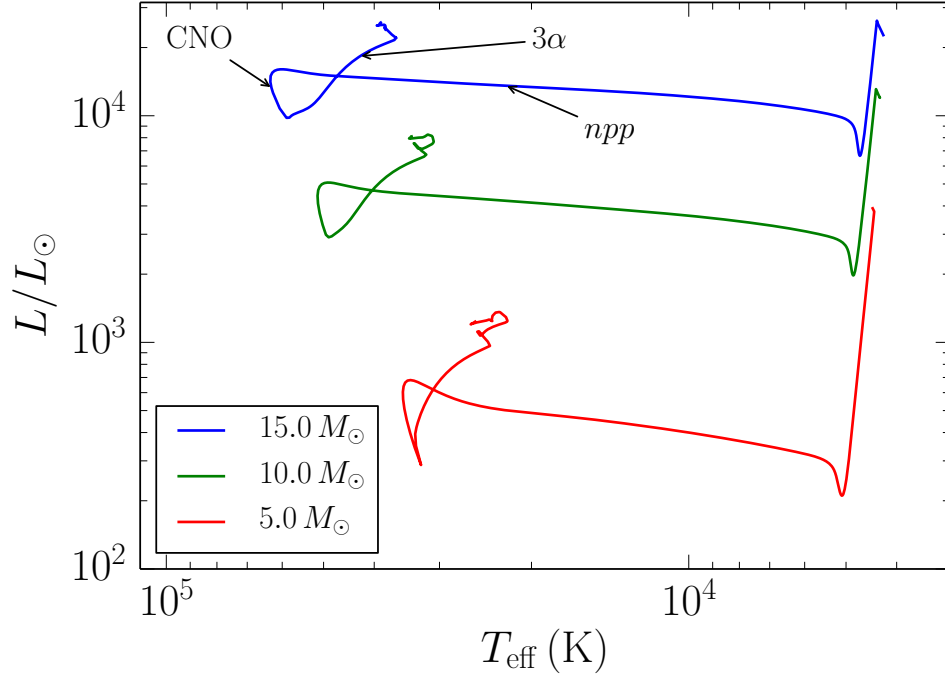


Figure 10: Tracks in the H-R diagram for stars with three different masses in a universe without stable deuterium. Initially, the stars have zero metallicity. The model employed here uses both the triple-nucleon reaction and CNO reactions. Labels on the $15 M_{\odot}$ curve correspond to different burning regimes, namely: *npp* when the core ^1H fraction falls to 99%; CNO when the reaction luminosity for CNO surpasses that of *npp*; and 3α when the core ^{12}C mass fraction rises to 1%.

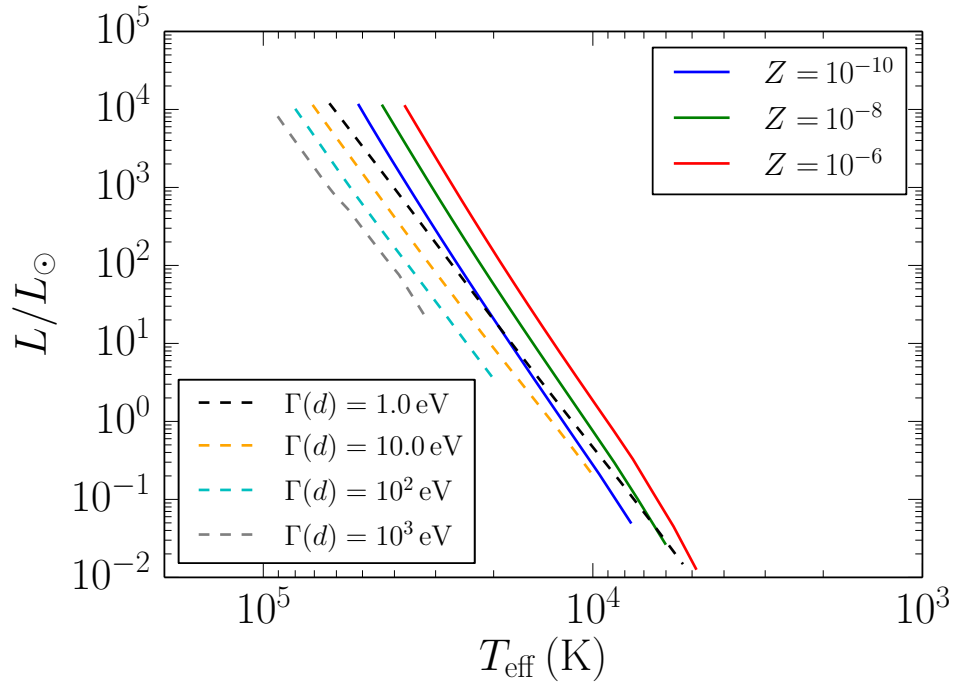


Figure 11: Zero-Age Main-Sequence for the different stellar models in a universe without stable deuterium. The masses range from $15 M_{\odot}$ down to $0.5 M_{\odot}$, depending on the models and parameters. The solid curves correspond to stars that only burn ${}^1\text{H}$ using the CNO cycle for metallicities $Z = 10^{-6}$ (red), 10^{-8} (green), 10^{-10} (blue). The dashed curves correspond to stars that employ the triple-nucleon reaction for widths $\Gamma(d) = 1 - 10^3$ (from right to left).

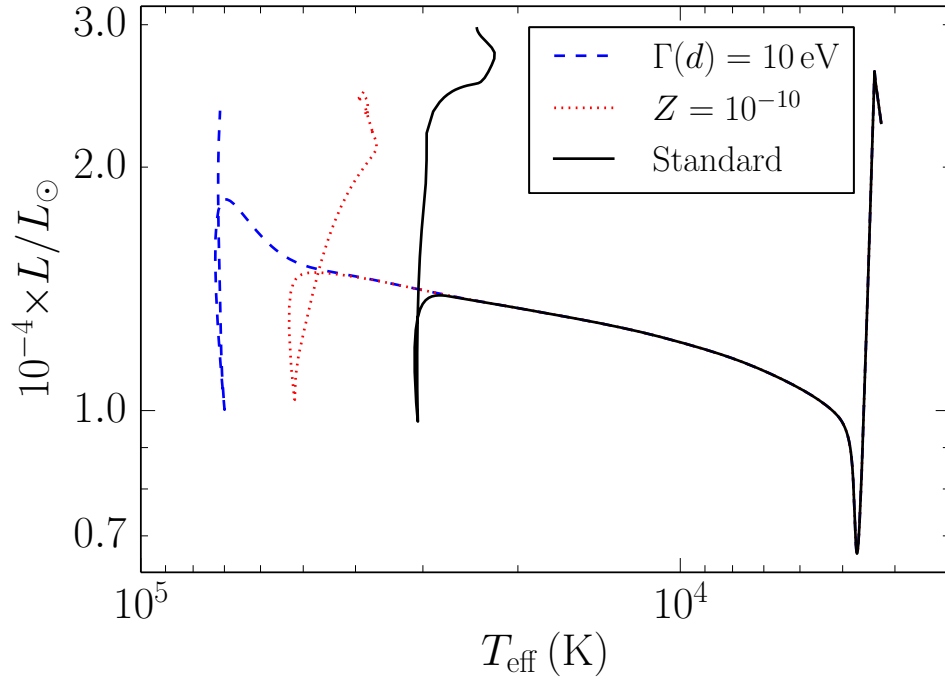


Figure 12: Evolutionary tracks in the H-R diagram for a star with mass $M_* = 15M_\odot$ operating with three different nuclear reaction chains for hydrogen burning. The three cases shown include the standard reaction chains in our universe (solid black curve), the CNO cycle with metallicity $Z = 10^{-10}$ (dotted red curve), and the triple-nucleon reaction with decay width $\Gamma(d) = 10$ eV (dashed blue curve).

In general, the slopes of the ZAMS are roughly parallel to each other for differing parameter values in a given model. Decreasing the metallicity Z in the CNO models, or increasing the decay width $\Gamma(d)$ in the triple-nucleon models, respectively, moves the ZAMS towards higher effective temperatures, while maintaining the same slope. The slope of the ZAMS provides a measure of the effectiveness of the nuclear reactions in supporting the star. Figure 11 shows that the main-sequences for the CNO models have somewhat larger slopes than those of the triple-nucleon models. More specifically, the slope of the ZAMS determines the degree to which increasing the stellar mass increases the power output of the star. Because the slope is larger for the CNO models, the reaction rates increase more rapidly with stellar mass (compared to the triple-nucleon models). In addition, as the reactions become less effective, either through decreasing metallicity or increasing decay width, the main-sequences shift to the left in the H-R diagram. The result is higher surface temperatures for the same luminosity.

We can also compare how the different nuclear processes considered in this paper affect the evolutionary tracks in the H-R diagram for individual stars. Figure 12 show the resulting tracks for stars with mass $M_* = 15M_\odot$ and three types of nuclear reaction chains. The black solid curve shows the evolutionary track for a star operating with all of the ordinary nuclear reactions in our universe. The dotted green curve shows the track for a star where hydrogen burning occurs only through the CNO cycle and where the metallicity is low ($Z = 10^{-10}$). Finally, the dashed blue curves shows the evolutionary track for a star burning hydrogen through the triple-nucleon process from Section 3.2, where the radiative decay width of deuterium is taken to be $\Gamma(d) = 10$ eV. For all of these cases, the higher order nuclear reactions (e.g., the triple-alpha process for helium burning) are assumed to be the same as in our universe. This assumption can be relaxed in future work, but the number of scenarios is large (and beyond the scope of this paper).

Along the sequence of models shown in Figure 12, from the ordinary reactions of our universe to triple-nucleon reactions with a large decay width, hydrogen burning becomes increasingly difficult. In all cases, however, the nuclear reaction rate must be large enough to provide pressure support for the entire stellar mass. As a result, the star must contract further to provide increasingly higher temperatures and densities in its core. The stars thus follow their radiative pre-main-sequence-like tracks farther to the left in the H-R diagram before adjusting downward to lower luminosities. This

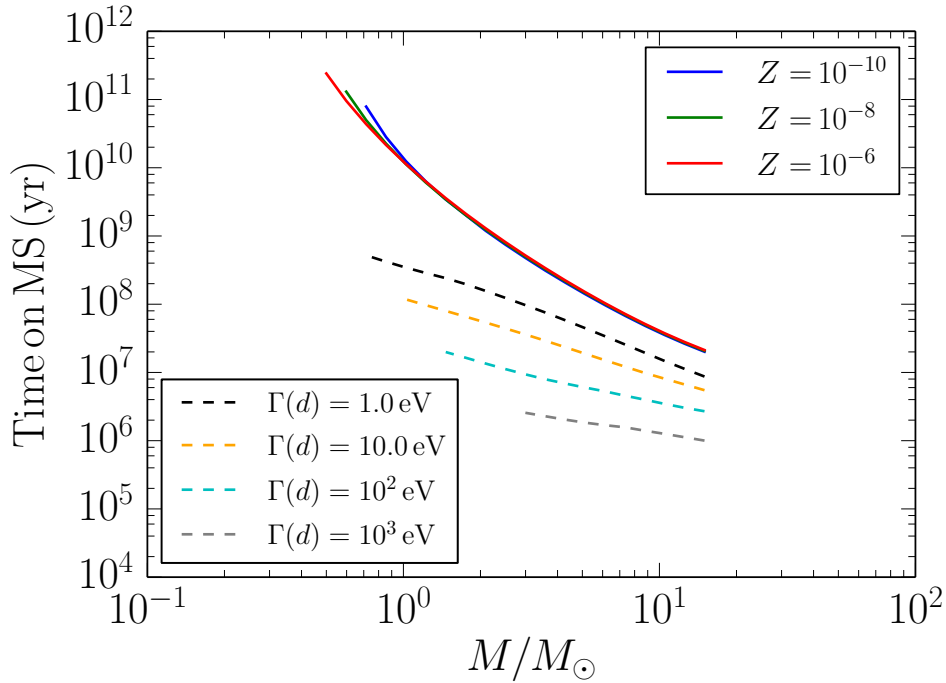


Figure 13: Main sequence lifetimes for stars with varying mass operating with the triple nucleon process (dashed curves) and with the CNO cycle (solid curves). The dashed curves for the triple nucleon process correspond to stars with decay widths $\Gamma(d) = 1$ eV (black), 10 eV (gold), 100 eV (cyan), and 10^3 eV (gray). The solid curves for the CNO cycle correspond to initial metallicities $Z = 10^{-6}$ (red), 10^{-8} (green), and 10^{-10} (blue).

behavior leads the stars to become hotter in effective temperature as well as in their cores. The stars also become somewhat brighter along this sequence of increasingly difficult hydrogen burning, but only by a factor of ~ 2 . The differences in effective temperature are more pronounced.

Figure 13 shows the main sequence (hydrogen burning) lifetimes for stars as a function of mass for the two types of nuclear processes considered in this work. For the sake of definiteness, the starting condition is defined as the time when the star burns 5% of the hydrogen (by mass) in its core, where the core is defined to be the inner 10% of the star (again by mass). The ending condition is defined as the time when the star burns 95% of the

hydrogen (by mass) in its core, or when the core reaches a point where more than 50% of the mass is sequestered in nuclei with $A > 5$. Note that the minimum mass for hydrogen burning varies with the nuclear process under consideration, so that not all masses are represented. The solid curves show the main sequence lifetimes for stars operating through the CNO cycle for metallicities in the range $Z = 10^{-6} - 10^{-10}$. The dashed curves show the lifetimes for stars operating through the triple nucleon process, where the decay width for deuterium is taken to be $\Gamma(d) = 1 - 10^3$ eV.

Figure 13 shows that the lifetimes for stars using the CNO cycle are relatively insensitive to the metallicity and are comparable to the lifetimes expected for stars in our universe (for a given mass). The lifetimes for stars using the triple nucleon process are systematically shorter, and vary significantly with the decay width $\Gamma(d)$. As the decay width increases, the lifetime of unstable deuterium decreases, and the stars have to contract further in order to achieve sustained nuclear fusion. This trend results in hotter stars that are brighter for a given mass and hence shorter-lived. In addition, stars operating through the triple nucleon process have central densities and temperatures comparable to those for helium burning stars in our universe. As a result, these stars tend to burn their helium into carbon (through the usual triple alpha process) at the same time they burn hydrogen into helium (through the triple nucleon process). These stars thus produce nuclei with $A > 5$ (especially carbon) and leave the main-sequence sooner. The smallest stars (with $\Gamma(d) = 1$ eV) live up to ~ 1 Gyr, perhaps long enough for accompanying planets to become habitable, whereas stars with larger widths have shorter lifetimes. Even if the hydrogen burning timescales are too short for life, however, the first generation of stars can produce carbon through the triple nucleon and triple alpha processes, so that later stellar generations will have enough carbon to operate through the CNO cycle.

5. Big Bang Nucleosynthesis without Stable Deuterium

The discussion thus far has assumed that a universe without stable deuterium will emerge from its early epochs with essentially no elements other than hydrogen. This assumption stands in contrast to the case of our universe, which processes about one fourth of its mass into helium, along with small (but nonzero) abundances of other light nuclei. The triple-nucleon reaction considered for stars could in principle instigate the production of

light nuclei during the BBN epoch. This section considers the early phases of evolution for universes without stable deuterium.

The triple-nucleon reaction relies on the presence of free neutrons. In the early universe, the plasma of charged leptons and neutrinos keeps the neutron-to-proton ratio in weak equilibrium, providing a sea of free neutrons for big bang nucleosynthesis. In our universe, the $n(p, \gamma)d$ and $d(p, \gamma)^3\text{He}$ reaction chain is primarily responsible for ^3He production. We have taken the *BURST* code [39] and substituted the individual deuterium reactions with the triple-nucleon reaction. In addition, we eliminated the deuterium isotope and all associated nuclear reactions from the network. Such a procedure does not preserve unitarity within the network (see Ref. [40] for a discussion of unitarity in BBN).

Figure 14 shows the evolution of the mass fractions of neutrons, protons (denoted ^1H), ^3H , ^3He , and ^4He , with decreasing co-moving temperature parameter T_{cm} (inversely related to scale factor) during BBN in a universe without stable deuterium. The values for the baryon-to-photon ratio and mean neutron lifetime are identical to those in our universe. We choose a value of $\Gamma(d) = 1.0 \text{ eV}$ for the decay width of deuterium. For high temperatures $T_{\text{cm}} \gtrsim 600 \text{ keV}$, the ^3H , ^3He , and ^4He abundances remain in NSE. At $T_{\text{cm}} \simeq 600 \text{ keV}$, the ^4He abundance begins to depart from NSE, as evidenced by the shoulder in the ^4He curve in Figure 14. The isotopes ^3H and ^3He remain in equilibrium longer, until T_{cm} reaches roughly 200 keV . Once the abundances depart from NSE, there is little increase in ^4He , a strict decrease in ^3H , and a provisional decrease in ^3He . These trends result from the triple-nucleon reaction being much too slow compared to the Hubble expansion rate to keep producing ^3He for eventual incorporation into a ^4He nucleus. In our universe, there is no such restriction. A sea of stable deuterium remains available (due to NSE) until the temperature falls well below $T_{\text{cm}} = 100 \text{ keV}$, when the deuterium undergoes out-of-equilibrium synthesis into ^4He .

We did not include the reaction $n + n + p \leftrightarrow ^3\text{H} + \gamma$. In our universe, $d(p, \gamma)^3\text{He}$ is the dominant channel for synthesis to nuclei with $A = 3$, so including the $2n(p, \gamma)^3\text{H}$ reaction in the BBN network would only modestly increase the final abundance of ^4He in Figure 14. The abundance of ^3H is larger than that of ^3He at the lowest temperatures in the plot. This is unusual as ^3He is the stable nuclear configuration for $A = 3$, and so we would expect a larger abundance of ^3He compared to ^3H due to equilibrium arguments. NSE is no longer obtained for $T_{\text{cm}} \lesssim 200 \text{ keV}$, and so the abundances of ^3H and ^3He evolve with the out-of-equilibrium nuclear rates. Transmutation

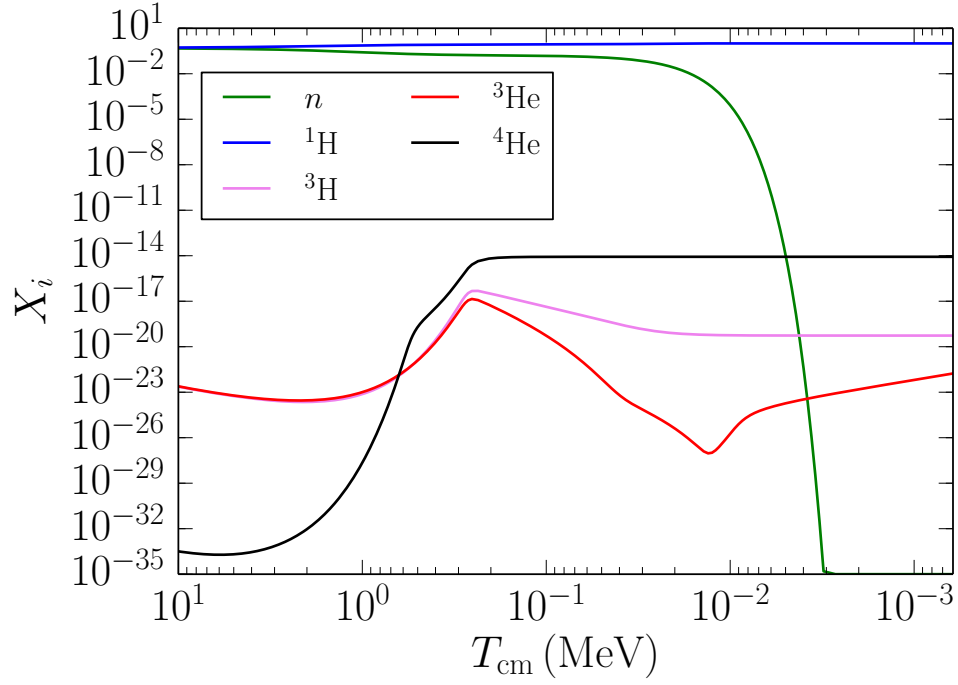


Figure 14: Time evolution of light element abundances (mass fractions) during Big Bang Nucleosynthesis for a universe without stable deuterium. The horizontal axis shows the background temperature T_{cm} of the universe as it decreases with increasing time. The model employed here uses the triple-nucleon reaction with $\Gamma(d) = 1.0 \text{ eV}$ to synthesize ${}^3\text{He}$ from two free protons and one free neutron. The largest mass fraction with $A > 1$ is ${}^4\text{He}$, which reaches a value of only $\sim 10^{-14}$. Mass fractions for lithium and beryllium are below the vertical scale of the plot.

of ${}^3\text{H}$ has three pathways: incorporation into ${}^4\text{He}$; beta-decay into ${}^3\text{He}$; or photo-dissociation into two neutrons and a proton. First, ${}^4\text{He}$ synthesis with ${}^3\text{H}$ occurs through the ${}^3\text{H}(p, \gamma){}^4\text{He}$ reaction. This reaction is slower than the principal pathway for ${}^4\text{He}$ synthesis with ${}^3\text{He}$, namely ${}^3\text{He}({}^3\text{He}, 2p){}^4\text{He}$. Second, ${}^3\text{H}$ has a lifetime of ~ 10 years, and so the associated rate is much smaller than the Hubble rate until later times. The rise in ${}^3\text{He}$ at $T_{\text{cm}} \sim 10\text{ keV}$ is due to the decay of ${}^3\text{H}$. Finally, the fact that deuterium, and its associated nuclear reactions, are absent in our BBN scenario, eliminates the pathway for ${}^3\text{H}$ destruction through the reverse channel of $d(n, \gamma){}^3\text{H}$. ${}^3\text{H}$ now must transmute directly into three nucleons, which would require a larger energy photon. However, this last point is moot as we did not include a ${}^3\text{H}$ version of the triple-nucleon reaction in our network. All told, the three pathways cannot transmute ${}^3\text{H}$ to ${}^3\text{He}$ within the span of time plotted on Figure 14.

The end result of these calculations is that BBN is nearly inert to the triple-nucleon reaction. The results in Figure 14 are presented for the particular decay width $\Gamma(d) = 1.0\text{ eV}$, but the value of $\Gamma(d)$ would have to be much smaller, so that deuterium is far more long-lived, in order for heavier nuclei to develop substantial abundances during the BBN epoch. As a result, if deuterium is unstable, the universe emerges from its early epochs with an almost pure hydrogen composition. In order for such a universe to become habitable, most nucleosynthesis must take place later in stellar cores (or other stellar environments).

6. Conclusion

This paper considers stellar evolution in universes in which deuterium has no stable bound state. Previous authors have argued that universes in this class would not allow for nucleosynthesis to take place due to the lack of a stable intermediate nucleus between hydrogen and helium. In contrast, we show that stars in deuterium-free universes can provide both energy and nucleosynthesis, and thus allow such universes to be potentially habitable.

6.1. Summary of Results

The results of this work, as summarized below, indicate that a number of different stellar processes can provide both luminosity and nucleosynthesis in the absence of stable deuterium:

[1] Stars can provide enough energy for habitability, over sufficiently long time scales, through the action of gravitational contraction. The time scale over which the luminosity is relatively large has a maximum value of a few Gyr for a stellar mass $M_* \sim 0.5M_\odot$ (see Figure 3). Somewhat larger stars have shorter lifetimes but their luminosity is more constant in time (Figure 5). Stars with initial masses below the Chandrasekhar limit can be supported by electron degeneracy pressure at the end of the gravitational contraction phase. These stars end their lives as white dwarfs. Stars with initial masses above the Chandrasekhar limit cannot be supported by degeneracy pressure and collapse at the end of their lives. These stars thus experience an explosive end state analogous to Type Ia supernovae. These explosions can provide heavy elements for subsequent stellar generations (Section 2.3).

[2] Under sufficiently hot and dense conditions, nucleosynthesis can take place through a class of triple-nucleon reactions (Section 3). Even with no stable state, a small population of deuterium nuclei will be present in stellar cores, although the forward reaction rates are not fast enough to reach nuclear statistical equilibrium (Section 3.1). This population of deuterium can interact with protons to produce helium, which is assumed to be stable. The deuterium nuclei also decay into free neutrons, which have larger reaction rates, and allow for a chain of nuclear reactions that produce helium (Section 3.2). The resulting triple-nucleon process is roughly analogous to the triple-alpha reaction through which helium is synthesized into carbon in intermediate mass stars. The central cores of ordinary stars can reach the temperatures and densities required for the triple-nucleon process to take place and thereby generate robust stellar luminosities (Section 3.3). Compared to stars burning hydrogen through conventional reactions, these stars are somewhat brighter and have higher surface temperatures (see Figure 7). The triple-nucleon process can also occur during the final collapse phases of stars evolving through gravitational contraction only (see Figure 4 and Section 2.3).

[3] Stars can also burn hydrogen through the CNO cycle. This process, which dominates energy production in stars more massive than the Sun, does not require deuterium, but does require a nonzero abundance of carbon. The CNO cycle can operate with only trace amounts of carbon, specifically, with metallicities as low as $Z = 10^{-10}$ for solar type stars (Section 4). This process can thus operate as long as a few stars per galaxy experience explosive nucleosynthesis (Section 2) in a previous stellar generation and/or if nucleosynthesis takes places via the triple-nucleon reaction (Section 3).

The resulting stars have properties similar to those in our universe, with a relatively normal main-sequence (Figure 9) and long lifetimes (Figure 13).

[4] The nuclear processes outlined above are not mutually exclusive, so that stars can derive energy through all of these channels over the course of their lifetimes (Section 4.3). In general, stars in universes without stable deuterium will begin their evolution with gravitational contraction. The central temperature increases with time, and eventually the stellar core becomes hot and dense enough for the triple-nucleon reactions to ignite and arrest further contraction. The conditions required for the triple-nucleon reaction to operate are similar to those required for helium burning, and hence carbon production, in ordinary stars. As a result, some of the helium produced via the triple-nucleon reaction will be burned into carbon through the triple-alpha process. When enough carbon builds up in the stellar core, energy generation through the CNO cycle can dominate (Figure 10). Note that the CNO cycle operates at lower central temperatures than the triple nucleon process. For subsequent stellar generations that are formed with nonzero carbon abundance, stars will burn their hydrogen through the CNO cycle before reaching the conditions where the triple nucleon process can take place.

[5] Although stellar nucleosynthesis can take place through alternate channels, Big Bang Nucleosynthesis is not effective in universes with no stable deuterium (Section 5). Compared to stellar conditions, the density of the universe is much lower during BBN, so that triple-nucleon reactions are highly suppressed. As a result, the universe ends up with only trace amounts of ${}^4\text{He}$ ($X_4 \sim 10^{-14}$) and even lower abundances of other nuclei (Figure 14).

6.2. Discussion

In our universe, the role played by stars varies with stellar mass. Low mass stars dominate the mass budget and live long enough to serve as hosts for habitable planets. High mass stars are rarer, but they dominate the generation of energy and the production of heavy elements necessary for life. In the alternate scenarios considered here, where deuterium has no stable state, high mass and low mass stars play analogous roles.

In the extreme limit where no (steady) nuclear processing takes place, a sharp division arises at the Chandrasekhar mass (where $M_{\text{Ch}} \approx 5.6M_{\odot}$ for stars composed of hydrogen). Stars of all masses contract as they evolve and produce energy through the loss of gravitational potential energy. Stars with $M_* > M_{\text{Ch}}$ evolve too rapidly to host habitable planets. They are also

too heavy to be supported by degeneracy pressure and eventually experience catastrophic collapse, so that their central temperatures and densities increase to enormous values. Under these extreme conditions, the absence of stable deuterium no longer enforces a bottleneck on nuclear processing and heavier elements can be produced. In contrast, stars with $M_* < M_{\text{Ch}}$ contract until they reach maximum temperatures and densities, where the values depend on stellar mass. These stars have highly diminished capacity for producing heavy elements, but they retain significant luminosities (comparable to stars in our universe) over long spans of time (up to billions of years).

In the case where the triple-nucleon process can operate, stars evolve much like those in our universe. The high mass stars are brighter, and hotter, and live for shorter spans of time. Stars of lower mass can live long enough to support habitable planets. Compared to stars in our universe, stars without stable deuterium must have a higher mass in order to achieve the same level of nuclear burning, and they have a shorter lifetime for a given mass. More specifically, the conditions required for hydrogen burning via the triple-nucleon process are comparable to those required for helium burning (carbon production) via the triple-alpha process. As a result, the minimum mass for sustained hydrogen burning, the brown dwarf limit, will occur at a higher mass than in our universe.³ At the other end of the mass spectrum, however, the maximum stellar mass is set by the onset of radiation pressure domination [20] and is not expected to change. The allowed range of stellar masses thus decreases.

This paper has explored a number of nuclear processes that allow stars to generate energy and produce heavy elements in the absence of stable deuterium, including explosive nucleosynthesis, triple-nucleon reactions, and the CNO cycle. The relative importance of these processes determines how stellar evolution ultimately occurs and depends on the mass difference between deuterium and its constituent particles. As deuterium nuclei become less stable, the nuclear processes considered in this paper become less efficient. For example, if deuterium nuclei are farther from stability, the radiative decay width $\Gamma(d)$ is larger, and stars require higher central temperatures for the triple-nucleon process to operate. In addition to making it more diffi-

³Note that the mass scale for the brown dwarf limit will depend on the parameters that characterize the instability of deuterium, e.g., the decay width $\Gamma(d)$ from Section 3.2.

cult for stars to burn hydrogen on the main-sequence, greater instability of deuterium reduces the efficacy of explosive nucleosynthesis. Although the CNO cycle operates without deuterium, it relies on carbon having a nonzero abundance, which in turn depends on the aforementioned nuclear processes involving deuterium. This paper argues that universes can remain habitable without stable deuterium. However, if deuterium nuclei were to become sufficiently unstable, the nuclear processes considered herein would become so inefficient that the universe would still end up lifeless. Such limits should be explored further in future work.

This paper assumes that deuterium is unstable but helium isotopes are bound. As a result, the universes under consideration here are roughly similar to our own. In order to quantify this issue, one can consider the possible parameter space for the Standard Model of particle physics where the quark masses are allowed to vary [3, 41, 42]. For particle physics models with two light quark species with different charges, like our own universe, such worlds will support analogs of protons, neutrons, and the corresponding composite nuclei. In order for hydrogen to have a stable isotope, the mass difference between the nucleons must satisfy the constraint $m_p - m_n < 7.97$ MeV, whereas the requirement for a stable carbon nucleus implies $m_n - m_p < 14.77$ MeV [42]. For comparison, the electron mass $m_e = 0.511$ MeV and the mass difference in our universe $m_n - m_p \approx 1.29$ MeV. According to this analysis, the quark masses must conspire to produce differences in nucleon masses that fall within a range of about 23 MeV. It is significant that all of these energies are small compared to the benchmark scale provided by the Higgs vacuum expectation value, which falls at ~ 246 GeV. The allowed window for nucleon mass differences to support stable nuclei (23 MeV) is thus relatively narrow compared to the Higgs scale (246 GeV), but still wider than the mass difference in our universe (1.3 MeV). In order to assess whether this allowed range for habitable universes is large or small, one needs the underlying probability distribution for the possible quark masses and other parameters of the Standard Model. These distributions are currently unavailable, but will hopefully become better understood in the future.

The results of this paper expand the range of potentially habitable universes to include some fraction of those without stable deuterium. Previous work [11] has already shown that stars can operate in universes where the strong force is more effective so that diprotons are bound. Variations in the strong force also influence the location of the carbon resonance that allows the triple alpha reaction to efficiently produce carbon in our universe. In

such universes, however, ^8Be can (sometimes) be stable, so that carbon can be produced via non-resonant reactions [43]. Still other work shows that stars can operate — with sufficiently long lifetimes and hot surface temperatures — over a wide range of values for the fine structure constant, the gravitational constant, and nuclear reaction rates [25, 26]. Taken together, these results indicate that stellar evolution has many different pathways, and that stars are robust enough to provide both energy and nucleosynthesis over a wide range of possible universes.

Acknowledgments: We would like to thank George Fuller, David Garfinkle, and Mark Paris for useful discussions. We also thank an anonymous referee for many useful comments that improved the paper. This work was supported by the JT Foundation through Grant ID55112: *Astrophysical Structures in other Universes*, and by the University of Michigan. Computational resources and services were provided by Advanced Research Computing at the University of Michigan.

References

- [1] B. J. Carr and M. J. Rees, *The Anthropic Principle and the Structure of the Physical World*, *Nature* **278** (1979) 611
- [2] J. D. Barrow and F. J. Tipler, *The Anthropic Cosmological Principle*, Oxford Univ. Press (1986)
- [3] C. J. Hogan, *Why the Universe is Just So*, *Rev. Mod. Phys.* **72** (2000) 1149
- [4] M. J. Rees, *Just Six Numbers*, Basic Books (2000)
- [5] A. Aguirre and M. Tegmark, *Multiple Universes, Cosmic Coincidences, and other Dark Matters*, *J. Cosmol. Astropart. Phys.* **01** (2005) 003
- [6] M. Tegmark, A. Aguirre, M. J. Rees, and F. Wilczek, *Dimensionless Constants, Cosmology, and other Dark Matters*, *Phys. Rev. D* **73** (2006) 3505
- [7] L. A. Barnes, *The Fine-Tuning of the Universe for Intelligent Life*, *Pub. Astron. Soc. Australia* **29** (2012) 529

- [8] A. N. Schellekens, *Life at the Interface of Particle Physics and String Theory*, *Rev. Mod. Phys.* **85** (2013) 1491
- [9] A. Vilenkin, *Unambiguous Probabilities in an Eternally Inflating Universe*, *Phys. Rev. Lett.* **81** (1998) 5501
- [10] A. H. Guth, *Inflation and Eternal Inflation*, *Phys. Rept.* **333** (2000) 555
- [11] L. A. Barnes, *Binding the Diproton in Stars: Anthropic Limits on the Strength of Gravity*, *J. Cosmol. Astropart. Phys.* **12** (2015) 050
- [12] F. J. Dyson, *Energy in the Universe*, *Scientific American* **225** (1971) 50
- [13] F. H. Shu, F. C. Adams, and S. Lizano, *Star Formation in Molecular Clouds: Observation and Theory*, *Ann. Rev. Astron. Astrophys* **25** (1987) 23
- [14] C. F. McKee and E. Ostriker, *Theory of Star Formation*, *Ann. Rev. Astron. Astrophys* **45** (2007) 565
- [15] K. L. Luhman, V. Joergens, C. J. Lada, J. Muzerolle, I. Pascucci, and R. White, *The Formation of Brown Dwarfs: Observations*, in *Protostars and Planet V*, ed. B. Reipurth, D. Jewitt, and K. Keil, Univ. Arizona Press (2007) 443
- [16] F. Palla and S. W. Stahler, *The Pre-Main-Sequence Evolution of Intermediate Mass Stars*, *Astrophys. J.* **418** (1993) 414
- [17] S. Chandrasekar, *An Introduction to the Study of Stellar Structure*, Univ. Chicago Press (1939)
- [18] D. D. Clayton, *Principles of Stellar Evolution and Nucleosynthesis*, Univ. Chicago Press (1983)
- [19] R. Kippenhahn and A. Weigert, *Stellar Structure and Evolution*, Springer (1990)
- [20] A. C. Phillips, *The Physics of Stars*, Wiley (1994)
- [21] M. Asplund, N. Grevesse, A. J. Sauval, and P. Scott, *The Chemical Composition of the Sun*, *Ann. Rev. Astron. Astrophys.* **47** (2009) 48

- [22] A. Frebel, J. L. Johnson, and V. Bromm, *The Minimum Stellar Metallicity Observable in the Galaxy*, *Monthly Notices Royal Astron. Soc.* **392** (2009) L50
- [23] E. W. Kolb and M. S. Turner, *The Early Universe*, Addison-Wesley Publishing (1990)
- [24] M. S. Smith, L. H. Kawano, and R. A. Malaney, *Experimental, Computational, and Observational Analysis of Primordial Nucleosynthesis*, *Astrophys. J. Suppl.* **85** (1993) 219
- [25] F. C. Adams, *Stars in other Universes: Stellar structure with different fundamental constants*, *J. Cosmol. Astropart. Phys.* **08** (2008) 010
- [26] F. C. Adams, *Constraints on Alternate Universes: Stars and habitable planets with different fundamental constants*, *J. Cosmol. Astropart. Phys.* **02** (2016) 042
- [27] B. Paxton, L. Bildsten, A. Dotter, F. Herwig, P. Lesaffre, and F. X. Timmes, *Modules for Experiments in Stellar Astrophysics (MESA)*, *Astrophys. J. Suppl.* **192** (2011) 3
- [28] B. Paxton, M. Cantiello, P. Arras, L. Bildsten, E. F. Brown, A. Dotter, C. Mankovich, M. H. Montgomery, D. Stello, F. X. Timmes, and R. Townsend, *Modules for Experiments in Stellar Astrophysics (MESA): Planets, Oscillations, Rotation, and Massive Stars*, *Astrophys. J. Suppl.* **208** (2013) 4
- [29] M. A. Wood, *Constraints on the Age and Evolution of the Galaxy from the White Dwarf Luminosity Function*, *Astrophys. J.* **386** (1992) 539
- [30] E. Bravo and G. Martinez-Pinedo, *Sensitivity Study of Explosive Nucleosynthesis in Type Ia Supernovae*, *Phys. Rev. C* **85** (2012) 055805
- [31] W. Hillebrandt and J. C. Niemeyer, *Type IA Supernova Explosion Models*, *Ann. Rev. Astron. Astrophys.* **38** (2000) 191
- [32] E. Livne and D. Arnett, *Explosions of Sub-Chandrasekhar Mass White Dwarfs in Two Dimensions*, *Astrophys. J.* **452** (1995) 62

- [33] F. E. Clifford and R. J. Tayler, *The Equilibrium Distribution of Nuclides in Matter at High Temperatures*, *Memoirs Royal Astron. Soc.* **69** (1965) 21
- [34] I. R. Seitenzahl, F. X. Timmes, A. Marin-Lafléche, E. Brown, G. Magkotsios, and J. Truran, *Proton-Rich Nuclear Statistical Equilibrium*, *Astrophys. J. Letters* **685** (2008) L129
- [35] A. Steyerl, J. M. Pendlebury, C. Kaufman, S. S. Malik, and A. M. Desai, *Quasielastic Scattering in the Interaction of Ultracold Neutrons with a Liquid Wall and Application in a Reanalysis of the Mambo I Neutron-Lifetime Experiment*, *Phys. Rev. C* **85** (2012) 065503
- [36] A. T. Yue, M. S. Dewey, D. M. Gilliam, G. L. Greene, A. B. Laptev, J. S. Nico, W. M. Snow, and F. E. Wietfeldt, *Improved Determination of the Neutron Lifetime*, *Physical Review Letters* **111** (2013) 222501
- [37] K. Nomoto, F.-K. Thielemann, and S. Miyaji, *The Triple-Alpha Reaction at Low Temperatures in Accreting White Dwarfs and Neutron Stars*, *Astron. Astrophys.* **149** (1985) 239
- [38] G. R. Caughlan and W. A. Fowler, *Thermonuclear Reaction Rates V*, *Atomic Data and Nuclear Data Tables* **40** (1988) 283
- [39] E. Grohs, G. M. Fuller, C. T. Kishimoto, and M. W. Paris, *Probing Neutrino Physics with a Self-Consistent Treatment of the Weak Decoupling, Nucleosynthesis, and Photon Decoupling Epochs*, *J. Cosmol. Astropart. Phys.* **5** (2015) 017
- [40] M. W. Paris, L. S. Brown, G. M. Hale, A. C. Hayes-Sterbenz, G. Jungman, T. Kawano, G. M. Fuller, E. Grohs, and S. Kunieda, *Toward a Self-Consistent and Unitary Reaction Network for Big-Bang Nucleosynthesis*, in *European Physical Journal Web of Conferences* **69** (2014) 00003
- [41] T. Damour and J. F. Donoghue, *Constraints on the Variability of Quark Masses from Nuclear Binding*, *Phys. Rev. D* **78** (2008) 014014
- [42] R. L. Jaffe, A. Jenkins, and I. Kimchi, *Quark Masses: An Environmental Impact Statement*, *Phys. Rev. D* **79** (2009) 065014

- [43] F. C. Adams and E. Grohs, *Stellar Helium Burning in Other Universes: A solution to the triple alpha fine-tuning problem*, *Astroparticle Phys.*, in press (2016), arXiv:1608.04690